The DOI for this manuscript is doi: 10.1175/JPO-D-13-0227.1

Some Dynamical Constraints on Upstream Pathways of the Denmark Strait Overflow

Jiayan Yang and Lawrence J. Pratt

Department of Physical Oceanography
Woods Hole Oceanographic Institution
Woods Hole, MA 02543, USA
(jyang@whoi.edu and lpratt@whoi.edu)

Revised manuscript submitted to: *Journal of Physical Oceanography*

July 1, 2014

Abstract: The East Greenland Current (EGC) had long been considered the main pathway for the Denmark Strait Overflow (DSO). Recent observations, however, indicate that the North Icelandic Jet (NIJ), which flows westward along the north coast of Iceland, is a major separate pathway for the DSO. In this study we use a two-layer numerical model and complementary integral constraints to examine various pathways that lead to the DSO and to explore plausible mechanisms for the NIJ's existence. In our simulations, a westward and NIJ-like current emerges as a robust feature and a main pathway for the Denmark Strait Overflow. Its existence can be explained through circulation integrals around advantageous contours. One such constraint spells out the consequences of overflow water as a source of low potential vorticity. A stronger constraint can be added when the outflow occurs through two outlets: it takes the form of a circulation integral around the Iceland-Faroe Ridge. In either case, the direction of overall circulation about the contour can be deduced from the required frictional torques. Some effects of wind stress forcing are also examined. The overall positive curl of the wind forces cyclonic gyres in both layers, enhancing the East Greenland Current. The wind-stress forcing weakens but does not eliminate the NIJ. It also modifies the sign of the deep circulation in various sub-basins and alters the path by which overflow water is brought to the Faroe Bank Channel, all in ways that bring our idealized model more in line with observations. The sequence of numerical experiments separates the effects of wind and buoyancy forcing and shows how each is important.

1: Introduction and Science Background

A large portion of the North Atlantic Deep Water (NADW) can be traced to overflows from the Nordic Seas across the Greenland-Iceland-Scotland Ridge (GISR, Figure 1). The overflow transport of the dense water mass, defined as those with a potential density higher than 27.8 kg m^{-3}, is about 6 Sv, which includes about 3 Sv through the Denmark Strait (DS, sill depth of 620m), 2 Sv via the Faroe Bank Channel (FBC, sill depth of 840m) and about 1 Sv over the Iceland-Faroe Ridge (IFR, maximum sill depth of 420m) (Hansen et al., 2008). Downstream of the sills, the overflowed water mass mixes vigorously with the ambient Atlantic Ocean water and forms the core of the NADW that flows southward as the lower limb of the Atlantic Meridional Overturning Circulation (AMOC, Price and Baringer, 1996). Both observations (Macrander et al., 2005; 2007; Eldevik et al., 2009) and numerical simulations (e.g., Köhl et al., 2007; Köhl, 2010; Serra, et al., 2010) indicate that the Denmark Strait Overflow (DSO) varies considerably on interannual time scales. Such variations result from atmospheric forcing and internal variability along the upstream pathways.

A marginal-sea overflow involves processes on both sides of the sill. This study focuses on the upstream pathways to the north of the GISR, and in particular those that are related to the DSO. In previous studies, the DSO pathways were identified mainly by comparing hydrochemical characteristics of water masses in the Nordic and Arctic Basins. Direct current measurements have been scarce. Swift et al. (1980) suggested that the water mass formed in the Iceland Sea supplies the DSO. Smethie and Swift (1989) proposed that the denser part of the DSO water originates from the Greenland Sea. Aagaard et al. (1991) and Buch et al. (1996) argued that water masses from the Arctic contribute to the overflow. Mauritzen (1996a,b) proposed that the Atlantic Water that has been transformed in the Nordic and Arctic Basins, the so-called Returned Atlantic Water, is the main component for the Denmark Strait Overflow. Rudels et al. (2002) analyzed observational data and concluded that the East Greenland Current (EGC) is the main pathway along which various components of the DSO water mass are transported (Figure 1 for the schematics). Their conclusion is supported by analyses of hydrochemical data (Tanhua et al., 2005; Jeansson et al., 2008). Even though the EGC has been considered as the main pathway in some previous studies, it has also been recognized that the water masses in the DSO consist of source waters from various Arctic and Nordic Basins and that its composition has evolved with time (Rudels, et al., 2003; Tanhua et al., 2005).

The prevailing view of the EGC being the dominant pathway for the DSO was questioned when measurements from moorings deployed for 3-years (1988-1991) off the northern Icelandic shelf and slope showed a persistent southwestward flow at about 500m depth, with a mean speed of about 10cm/s, toward the Denmark Strait (Jonsson, 1999). Jonsson and Valdimarsson (2004) confirmed the existence of this current based on shipboard observations made in November 2001 and 2002. The existence of the Icelandic branch of the DSO was further confirmed by extensive surveys along the northern Icelandic shelf and slope in 2008 and 2009 (Våge et al., 2011). They observed that this branch, which they called the North Icelandic Jet (NIJ), is centered on the 600m isobath (approximately the sill depth in Denmark Strait) and that its origin can be traced to the region northeast of Iceland (Figure 1). Våge et al. (2013) analyzed a new set of observations made in August 2011 and 2012 and showed that about 70% of the DSO water approaches the sill along the Iceland continental slope and it is supplied by two separate currents, namely the NIJ and a separated branch of the EGC. (The latter has been diverted eastward from the Greenland continental slope upstream of the sill.) Våge et al. (2013) suggested that eddy fluxes associated with a baroclinically unstable EGC are responsible for the EGC separation. Such a separation, as noted by Våge et al. (2013), also occurs in rotating hydraulics models (e.g., Helfrich and Pratt, 2003; Yang and Price, 2000) when an outflowing current approaches a shallow sill. The bifurcation of a southward WBC in a hydraulics model is mostly determined by the layer thickness upstream of the sill. It occurs when the layer thickness of the source water (h_2) is affected the shoaling bathymetry and the flow along Greenland's coast no longer can maintain its course toward Denmark Strait along f/h_2 isolines. If the WBC is flowing along isobaths that are deeper than the sill depth, it tends to detach from the western boundary and then approach the sill on the eastern side. The topographic slope leading to the sill makes the eastern boundary behave like a dynamical western boundary. If the approaching WBC is along isobaths shallower than the sill depth, it usually continues southward along the western boundary toward the sill. In the EGC case, it is expected, in a hydraulics model, that the portion of the flow on the inner slope along isobaths that are shallower than the sill depth would continue to approach the sill as a WBC while the flow along deeper isobaths detach from the western boundary. It is possible that the two mechanisms (eddy and topographic beta) are linked. Våge et al. (2013) demonstrated convincingly that the NIJ is an independent pathway that co-exists with the separated EGC and that the NIJ accounts for roughly half of the DSO transport. In a study using an idealized model, Våge et al., (2011) suggest that the NIJ could be fed entirely by water that has been cooled in the Iceland Sea, and that has originally made its way into the Nordic Seas via the North Icelandic Irminger Current, which flows at the surface northwestward through the DS and around Iceland. The numerical model domain consisted of only a small portion of the Nordic Seas.

In this study, we use a two-layer marginal-sea overflow model (Yang and Pratt, 2013) to investigate some dynamical constraints on the DSO pathways with the main focus on the existence of the NIJ. We do not address where the DSO source water is formed but rather some basic dynamical processes and balances that relate to the DSO pathways regardless of the origin of the source water. The two-layer framework is idealized, but it accounts for the basic exchange properties between the Atlantic Ocean and the Nordic Seas across the GISR (e.g. Dickson et al., 2008 and Pratt and Whitehead, 2008) and it provides a good setting for intuition building. The numerical model is described in Section 2 and this is followed in Section 3 by discussion of some simulations that lack wind forcing and produce an NIJ-like current. In Section 4 we address the apparently robust nature of this result using circulation integrals. This discussion will emphasize the importance of the 'island' geometry of Iceland. Wind stress forcing leads to a more realistic lower layer circulation while preserving the NIJ and this is described in Section 5. A summary is given in Section 6.

2. A two-layer marginal-sea overflow model

We use a primitive equation, two-layer model (Yang and Pratt, 2013) in this study. Both layers are active and so the model includes the barotropic and the 1st baroclinic modes. The thickness of either layer is allowed to become zero (*i.e.*, outcropping of the lower or grounding of the upper layer). A marginal-sea overflow has been considered in many studies as a two-layer exchange over a ridge between two basins. Thus two-layer ocean models have been one of the most commonly used tools in such studies (see Pratt and Whitehead, 2008 for a comprehensive review). It is assumed that the upper layer is filled by buoyant water masses of either high temperature or low salinity while the lower layer contains dense water masses that have been formed in the marginal sea by surface air-sea fluxes. In the Nordic Seas, a potential density of 27.8 kg m^{-3} is often used to separate the upper and lower layers.

While the deep Nordic Seas are filled with a rather uniformly cold dense water mass, the upper layer in the Nordic Seas contains a wide range of water masses, including low salinity and cold Arctic Ocean water along Greenland's coast and warm and saline Atlantic Water off Norway. These waters are modified by air/sea interaction as they circulate. In our two-layer model, horizontal changes in water properties are contained only in variability of the upper layer thickness and the ability of the lower layer to outcrop, so features such as the gradual densification of the Atlantic Water as it circulates around the basins cannot be captured in a realistic way. Nevertheless, we anticipate that the model will provide fundamental information and insight concerning preferred deep pathways towards the Denmark Strait. The simplicity and transparency in dynamics are its main advantage over OGCMs. The potential density $\sigma_\theta =$ 27.8 kg m^{-3} is often used to separate the inflowing and outflowing layers, and we think of this surface as more or less coinciding with our two-layer interface.

Our model is governed by the following set of equations:

$$
\begin{aligned}
&\frac{d\vec{u}_1}{dt} + f\vec{k}\times\vec{u}_1 = -g\nabla\eta - A\nabla^4\vec{u}_1 + (1-H(h_2))\vec{F}_1 + \frac{\vec{\tau}_{wind}}{\rho h_1} \\
&\frac{d\vec{u}_2}{dt} + f\vec{k}\times\vec{u}_2 = -g\nabla\left(\eta - \frac{\Delta\rho}{\rho_2}\eta_2\right) - A\nabla^4\vec{u}_2 + \vec{F}_2 + (1-H(h_1))\frac{\vec{\tau}_{wind}}{\rho_2 h_2} \\
&\frac{\partial\eta}{\partial t} + \nabla\cdot(h_1\vec{u}_1 + h_2\vec{u}_2) = 0 \\
&\frac{\partial h_2}{\partial t} + \nabla\cdot(h_2\vec{u}_2) = w_e
\end{aligned}
\qquad (1)
$$

where (u_n,v_n) and h_n are velocity and layer thickness in the n[th] layer (n=1, 2 for the upper and lower layers respectively), η and η_i are the sea surface and the layer interface heights from the their initial conditions respectively, $A = 1 \times 10^{11} m^4 s^{-1}$ is a biharmonic viscosity, $\vec{F}_n = \frac{\gamma |\vec{u}_n| \vec{u}_n}{h_n}$ is the bottom drag on the n[th] layer (where $\gamma = 0.005$ is a quadratic bottom drag coefficient) and $\Delta\rho = 1/3\ kg/m^3$ is the water density difference between two layers. The biharmonic form of lateral friction is used since it suppresses grid-size numerical instability effectively. The model allows outcropping of the lower layer ($h_1=0$) or grounding of the upper layer ($h_2=0$). The lower layer is exposed to wind stress wherever it outcrops. Likewise, the bottom stress is applied to the upper layer when it grounds. These are handled by the Heaviside Step Function $H(h_i)$ ($H(h_i)=1$ if $h_i > 0$, and $H(h_i)=0$ if $h_i \leq 0$. The model is not forced explicitly by surface buoyancy fluxes, instead a diapycnal velocity, w_e, is used to represent a main effect of buoyancy forcing - the formation of deep water. This cross-interface velocity is also referred in the paper as a 'downwelling' for mass transport from the upper to the lower layer and a 'upwelling' for an opposite transport.

The model uses both idealized and realistic bathymetry (Figure 1). In all experiments with a realistic topography, the model extends from 55˚N to 80˚N and has a resolution of 1/12˚ in the meridional direction and 1/6˚ in the zonal direction. All lateral boundaries are closed and areas shallower than 200m are set to be land[1]. We use a steady wind stress that is averaged from a 23-year (1988-present) daily climatology (Yu et al., 2008). The model uses a staggered C-grid and a small time step of 6 seconds, which provides numerical stability for fast barotropic waves.

[1] The DSO pathways, which are centered along 600-700m isobaths, are not sensitive to excluding shelf seas that are shallower than 200m.

Simulations that use idealized bathymetry have both open and closed boundaries. For the open boundary condition, we assume the inflow is geostrophic and prescribe the inflow velocity and pressure across the gap. The type of the boundary condition in each experiment will be described when the simulation is presented.

3. The DSO pathways

Our objective is to identify factors that influence the deep pathways, including the NIJ, from the upstream source regions to the DS. For now we will refer to any modeled deep westward flow along the north Iceland coast as the 'NIJ', with the caveat that particular features such as volume flux and linkage with upstream currents may differ from observations and may vary between numerical experiments. The DSO is a topographically restricted and hydraulically controlled flow (Käse and Oschlies, 2000; Käse et al., 2003; Wilkenskjeld and Quadfasel, 2005). The Nordic Seas Overflow, including the DSO, is primarily driven by a buoyancy flux (Hansen et el., 2008). The wind-stress forcing modulates overflow variability (e.g., Biastoch et al., 2003; Köhl, et al., 2007; Nilsen et al., 2003; Serra et al., 2010). In this section we will discuss first the DSO pathways in circulations that are forced by water-mass sources and sinks, with no wind.

Previous studies indicate that there are likely multiple origins of the DSO source water and we will consider the outcome of varying the origin later in this paper. We first wish to establish a benchmark (EXP-1) in which we determine the draining pathways that arise when the dense water source is turned off [$w_e=0$ in (1)] and the outflow occurs as a result of the sudden release of a pre-existing volume of dense water. In the experiment setup, the dense water initially fills the basin to the north of the GISR to the depth level that is 50m below the sea surface (Figure 2). The lighter water in the upper layer fills the rest of the model domain, *i.e.*, the entire basin to the south of the ridge and the upper 50m in the Nordic Seas. When this volume is released, the initially piled-up dense water floods across the ridge and descends into the deep ocean. This flow adjustment process is similar to the classical lock exchange experiment in a rotating system (Pratt and Whitehead, 2008). Similar numerical experiments have been used to examine the Nordic Seas overflow pathways (Käse et al., 2009) and to assess the effective capacity of the dense-water reservoir (Yang and Pratt, 2013).

Figure 3a shows the sea surface height (SSH) and upper layer velocity at the end of 1-year model run. The lighter water in the upper layer flows northward into the Nordic Seas through passages between Iceland and Scotland and along the eastern side of the Denmark Strait. A southward East Greenland Current flows on the western side of the Denmark Strait. A prominent feature in the surface circulation in the Nordic Seas is a basin-wide cyclonic rim current. The flow is very weak in the interior. The dense water masses in the deep basins are stored within closed geostrophic contours and thus somewhat buffered from the boundary currents, a feature explored in more depth by Yang and Pratt (2013). The circulation in the lower layer (Figure 3b) is dominated by an anti-cyclonic boundary current in the Nordic Seas. The circulation in the deep Greenland Sea is very weak and there is no deep expression of the EGC. The boundary current draws water mass mainly from the Lofoten Basin, which seems to be consistent with the study of Isachsen et al. (2007). The dense water moves southward along the continental slope off Norway and feeds the Faroe Bank Channel overflow. A branch of this deep current flows toward the west along the 600-800m isobaths north of the GISR and exits through Denmark Strait. In the vicinity of Iceland, this westward flow resembles the North

Icelandic Jet. But it should be noted that the westward jet in Exp-1 extends far to the east of Iceland, whereas the observations of Våge et al. (2013) suggest a termination point along the north Iceland coast, a feature supported by four independent surveys. Our model NIJ becomes more realistic when wind stress is added (to be discussed in Section 5).

The dam-break experiment shows that a westward boundary current along the North Iceland coast is the dominant pathway for the DSO in a drainage overflow without renewal of deep water. In reality, the overflow source water is replenished by winter convection, so we next consider the simplest of cases with a source of overflow water. In EXP-2 a uniform diapycnal flux, i.e., w_e=*constant*>0 (positive for a downward flux from upper to lower layer), is applied over the entire Nordic Seas to the north of the GISR (within the red contour line shown in Figure 4a). The total diapycnal flux is specified to be 6 Sv initially (the same for all experiments that uses w_e). (In order to close the overturning circulation, a region of negative w_e is imposed at southwestern corner of the model domain south of the GISR.) The wind stress is turned off as in the previous experiment.

The downwelling results in outcropping of the lower layer in the interior Nordic Seas. The area within the black contour in Figure 4a indicates the area of outcropping at the end of the 10th year simulation. The downwelling w_e is turned off whenever the lower layer outcrops. So the net downwelling is less than the initial 6 Sv. At the end of the 10th year in EXP-2, the downwelling occurs only in the area between the red and black lines shown in Figure 4a. Figure 4b shows that the overall rim circulation in the lower layer is again anti-cyclonic. The southward eastern boundary current supplies dense water to both FBC and the DS. The overall circulation pattern is similar to that in the dam-break experiment (Figure 3b). A noticeable difference is the existence of a northward western boundary current in the lower layer of the

Greenland Basin. This deep current is opposite in flow direction to the EGC in the upper layer and is associated with an anti-cyclonic Greenland Sea gyre that is forced by vortex squashing induced by the downwelling w_e. The lower layer circulations in the other two major deep basins (Norwegian and Lofoten) are also anti-cyclonic. In areas between the black and red lines in Figure 4a, the vortex squashing forces flows across f/h contours from high to low PV. In the area where the lower layer outcrops (within the thick black contour in Figure 4a), w_e is zero and the flow is mainly along f/h contours. The flows around the GISR are similar to that in the dam-break experiment. The NIJ in the lower layer in this simulation is robust and flows westward along the 500-800m isobaths toward the Denmark Strait. In fact, the DSO transport in this experiment is supplied almost completely by the NIJ.

In reality the water-mass transformation is certainly not uniformly distributed in the Nordic Seas. The DSO water is a composition of water masses from multiple origins according to analyses of hydrochemical data (Tanhua et al., 2005). We would like to examine whether the NIJ's existence depends on where and how the DSO source water is formed. Intuitively, one would expect that an overflow pathway is a direct conduit from the source to the sill and thus is tied to the source's location. For instance, the EGC would be an expected pathway if the source of the DSO water is in the Greenland Sea. But as we will show next, the NIJ's existence is rather insensitive to where the DSO source water is formed.

In the 3rd experiment (EXP-3), a localized water-mass flux from the upper to lower layer is placed on the continental slope off the east coast of Greenland (the location of downwelling is indicated by the purple oval in Figure 5a). As in previous experiments, the wind stress is turned off. The velocity in the lower layer is shown in Figure 5a. The source water, which is injected into the lower layer on the continental slope of the Greenland Sea, forms a southward western boundary current within the Greenland Sea. But instead of continuing southward to the Denmark Strait, it recirculates within the Greenland Sea and flows across the Mohn Ridge into the Lofoten and Norwegian Basins. There are strong anti-cyclonic circulations in these two basins. The flow along the Jan Mayen Ridge is northward as a part of the anti-cyclonic gyre in the Norwegian Basin. There are flows from the northern Greenland Sea southward along the continental slope off Spitsbergen and Norway into the Lofoten and Norwegian Basins. This eastern boundary current continues southward and splits, with one branch feeding the overflow through the Faroe Bank Channel and second feeding the westward NIJ along the 600-800 isobaths to the north of Iceland-Faroe Ridge. The NIJ is the dominant source for the Denmark Strait Overflow. The East Greenland Current just north of the Denmark Strait is weak even though the source of the low-layer water is placed in the Greenland Sea. Some features of EXP-3, including the sense of deep circulation in the 3 major basins, differ from observations, the same as in the previous two experiments without wind-stress forcing. The important point is that, despite these differences, the NIJ is present.

We have conducted several additional source/sink-driven experiments by moving the water-mass source to different locations or by specifying the source as a southward inflow boundary condition across the Fram Strait from the Arctic Basin. The NIJ always emerges as the dominant pathway for the Denmark Strait Overflow. In fact, we have not been able to simulate a Nordic Seas overflow that does not have the NIJ as its main pathway for the DSO in all of our source- and sink-driven experiments. The NIJ is apparently a robust and permanent feature, at least in model runs that lack wind forcing. We now show that its existence in the model is consistent with some constraints, one of them quite powerful, involving potential vorticity dynamics and circulation.

4. Plausible mechanisms for the NIJ

In this section we will discuss two integral constraints that identify conditions that are favorable to the existence of the NIJ-like current. The first is a circulation integral that extends around a contour C that rims the Nordic Seas (Figure 6). The basin may be closed to the north or may contain an opening that acts as a potential source of overflow water from the Arctic. In terms of dynamics, a key question that will arise is whether the overflow source water originates from the deeper portions of basin, and therefore has relatively low potential vorticity (PV), or whether it originates from shallower coastal areas. The tendencies predicted by the first constraint are thus sensitive to the location of the diapycnal velocity w_e, and especially to whether it is concentrated in the interior of the basins or near the boundaries. We will consider both situations. The second constraint is stronger and derives from the circulation around the 'island' contour C_I that circles Iceland and the Iceland-Faroe Ridge (Figure 6). This integration constraint is not sensitive to the location of the diapycnal velocity w_e in the Nordic Seas. The details of these two integration constraints are discussed next.

4.1: A Basin Circulation Integral Constraint

In a source- and sink-driven flow, the circulation around any closed contour C is constrained by the vorticity advection across C as well as the tangential stresses acting on C. Pratt (1997), Yang and Price (2000, 2007) and Helfrich and Pratt (2003) used circulation integrals to infer flow directions around closed geostrophic contours or lateral boundaries in semi-enclosed marginal seas. Yang (2005) and Karcher et al. (2007) applied this constraint to explain that the circulation in the Atlantic Water Layer in the Arctic is cyclonic in part due to a net positive transport of PV from sub-Arctic basins. These integral constraints can provide information about the average direction of tangential flow around *C*, but they do not necessarily determine the direction of flow along any a particular segments of *C*. The constraints tend to be simplest when applied along slippery, vertical walls since fluxes across *C* are then zero. For the more realistic case of sloping topography, an advantageous choice of *C* is a closed f/h_2 contour (provided that the contour does not wander out of the domain of interest), with h_2 chosen to correspond to the depth at which knowledge of the direction of circulation is desired.

We begin by writing the steady version of the lower-layer momentum equation (see Eq. 1) as:

$$(f+\zeta_2)\vec{k}\times\vec{u}_2 = -\nabla[g\eta_1 + (g\Delta\rho/\rho)\eta_2 + \frac{1}{2}|\vec{u}_2|^2] + \vec{F}_2 + (1-H(h_1))\frac{\vec{\tau}_{wind}}{\rho h_2} \qquad (2)$$

Note that we have disregarded the biharmonic friction term, which is included in the numerical model for numerical stability but is generally dominated by the bottom drag term in the lower layer. We now make the following approximations: First, we assume that the relative vorticity ζ_2 is much smaller in magnitude than *f*; that is, the Rossby number is small. We also assume that $|\eta_2| << h_2$, meaning that variations in the lower layer thickness are dominated by variations in topography. Finally we assume that *f* is constant. We then consider a closed contour *C* along which the lower layer does not outcrop. Integrating (2) about *C* yields:

$$\oint_C f\vec{u}_2\cdot\vec{n}\,ds = \oint_C \vec{F}_2\cdot\vec{l}\,ds \qquad (3)$$

where $\vec{F}_2$ is the sum of external forces, including friction and wind stress, $\vec{n}$ and $\vec{l}$ are unit vectors that are aligned in the normal and tangential direction to *C*. Equation (3) states that the divergence of the advection of planetary vorticity across *C* is balanced by the integral of tangential forces acting around *C*. The wind stress will need to be included in $\vec{F}_2$ if the lower layer outcrops along *C*.

Consider a basin (Figure 6) from which dense water is drained by two straits, analogous to the Denmark Strait (DS) and Faroe Bank Channel (FBC), and possibly fed from a third strait to the north, analogous to the Fram Strait (FS). The 620m DS sill depth also lies at the approximate observed mean depth of the NIJ, so we choose the corresponding isobaths (or perhaps one slightly deeper) as our integration contour *C*. Since the sill depth of the FBC (about 840m) and the depth of the Fram Strait are both greater than 620m, we amend *C* so that it cuts across these two passages, as shown by the dashed segments in Figure 6. The contour passes continuously across the upstream entrance of the DS, so no cut is needed there. Application of (2) about this contour leads to

$$\oint_{C_{int}+C_{FBC}+C_{FS}} f\vec{u}_2 \cdot \vec{n}ds = \oint_{C} \vec{F}_2 \cdot \vec{l}ds \tag{3a}$$

where C_{FBC} and C_{FS} denote that segments of *C* that cross the Faroe Bank Channel and Fram Strait, and C_{int} denotes the remaining portion of *C*. All of C_{int} lies along 620m, or slightly deeper isobaths.

We next assume that the lower layer thickness is approximately a constant ($=H_{int}$) along the isobaths-following portion C_{int}, which would be consistent with quasigeostrophic flow along this part of the contour. Across the short segments C_{FBC} and C_{FS}, we assume that the depth is constant and the corresponding layer thicknesses H_{FBC} and H_{FS} are then also approximately constant. (This approximation is tantamount to the assumption that the deep entrance to the straits in question has a rectangular cross section and that the difference in interface height across the entrance is small compared to the lower layer depth.) If we further assume that *f* does not vary substantially over the latitude range of the basin, then (3) may be rewritten as

$$\frac{f}{H_{\mathrm{int}}}\oint_{C_{\mathrm{int}}} H_{\mathrm{int}}\vec{u}_2\cdot\vec{n}ds+\frac{f}{H_{FBC}}\oint_{C_{FBC}} H_{FBC}\vec{u}_2\cdot\vec{n}ds+\frac{f}{H_{FS}}\oint_{C_{FS}} H_{FS}\vec{u}_2\cdot\vec{n}ds=\oint_{C}\vec{F}_2\cdot\vec{l}ds$$

or,

$$\frac{fQ_{\mathrm{int}}}{H_{\mathrm{int}}}+\frac{fQ_{FBC}}{H_{FBC}}-\frac{fQ_{FS}}{H_{FS}}=\oint_{C}\vec{F}_2\cdot\vec{l}ds \qquad (4)$$

where Q_{FBC}, $Q_{FS,}$ and Q_{int} are the volume fluxes through the Faroe Bank Channel and Fram Strait, and across C_{int}. (The terms on the left, which were originally expressions of planetary vorticity advection across a contour (as expressed in Eq. 2) have been rewritten so as to represent fluxes of planetary PV.) All three *Q*-values are positive and the negative sign in front of Q_{FS} is due to the fact that the flux is inward as it crosses *C*. Note that C_{int} is not necessarily equal to the volume flux through the Denmark Strait since this outflow may also draw on sources from shallow coastal regions lying outside of *C*. In developing (4) we have stated a number of assumptions that could be challenged. For example, one might question the neglect of relative vorticity where *C* gets close to the DS sill. We also neglect the contribution from wind stress in areas where the low layer outcrops. Nevertheless, (4) captures the basic ingredients of the circulation balance that occurs when vorticity fluxes are dominated by planetary vorticity and variations in *f* are weak.

Since the deep basin may also be fed from above by interior deep convection

$$Q_{int} + Q_{FBC} \geq Q_{FS}.$$

Equation (4) then implies

$$\oint_C \vec{F}_2 \cdot \vec{l}\,ds = \frac{fQ_{\text{int}}}{H_{\text{int}}} + \frac{fQ_{FBC}}{H_{FBC}} - \frac{f(Q_{FBC}+Q_{\text{int}})}{H_{FS}} = fQ_{\text{int}}\left(\frac{1}{H_{\text{int}}} - \frac{1}{H_{FS}}\right) + fQ_{FBC}\left(\frac{1}{H_{FBC}} - \frac{1}{H_{FS}}\right). \qquad (5)$$

Since the Fram Strait and Faroe Bank Channel are both deeper than the Denmark Strait, we expect $H_{int} < H_{FBC}$ and $H_{int} < H_{FS}$. Thus the right-hand side of (5) is positive, meaning that the tangential stress $\vec{F}_2 \cdot \vec{l}$ around C must therefore also be positive on average. If the stress vector is largely due to bottom drag, in either linear form[2] or quadratic form, the circulation around C must on average be negative, or anticyclonic. If the lower layer outcrops along any portion of C, the wind stress may then contribute to $\vec{F}_2$ and the outcome could be different.

The presence of average anticyclonic flow around the 620m isobaths of the Nordic Seas does not in itself imply the presence of a westward NIJ. However, the presence of the East Greenland Current, which flows in a cyclonic sense, does strengthen the requirement for anticyclonic flow elsewhere around C in order to satisfy the integral constraint. This would strengthen the argument for westward flow along the North Iceland slope, but this is as far as this argument can be pushed. It should also be recognized that the sinking that feeds the overflows could occur dominantly outside of C, a situation we will investigate in Section 4.2.

Support for the tendencies predicted by (5) can be gained from a pair of idealized experiments with simplified geometry (Figure 7). In both experiments we use a model domain of 500×800 km with a depth of 2500 m in the deep basin and of 1250 m at the sill (Figure 7a). There is just one draining strait in either case, so we set Q_{FBC}=0 in (4) and (5). We use a reduced-gravity model version of (1) by setting the upper layer velocity and surface pressure

---

[2] Although our governing equations do not resolve bottom Ekman layers, a linear bottom drag law would produce a cross-isobath flux that could be made consistent with a bottom Ekman layer through the correct choice of the coefficient in the linear bottom drag law. This is discussed in Pratt (1997).

gradient to be zero. The model uses Cartesian coordinates and has a resolution of 5km. A water-mass source for the lower layer is introduced either as downwelling from the upper to lower layer in the northwestern corner (Figure 7b) or as an inflow through the northern boundary (Figure 7c). An outflow is specified in the southern boundary so that the mass flux into the lower layer is balanced. We are primarily interested in upstream pathways connecting the source to the DSO. In both forcing types, the source water is introduced in the northern basin and needs to overflow a shallower strait to the southern basin.

In the first idealized experiment (‘*IDL-1*’), the water-mass source in the northern basin is completely due to a specified downwelling (w_e>0) in Eq. (1). Thus Q_{FS}=0 in (4) and the overall rim circulation about the basin is predicted to be anti-cyclonic. As shown in Figure 7b, the downwelling forces a strong local recirculation and the boundary current around the northern basin is anti-cyclonic. The water mass approaches the shallow strait as an NIJ-like current along the shelf and slope of the model’s `Iceland’. These features are qualitatively similar to those source- and sink-driven experiments that use realistic bathymetry (Figure 4b and 5a).

The consequences of Eq. (4) are apparent in a plot of the cumulative friction, integrated following a contour *C* that starts at the southeastern corner in the northern basin and proceeds cyclonically along the 1500m isobath:

$$T(s) = \int_0^s F(l)dl. \qquad (6)$$

Here *F* is the tangential component of the total lower-layer friction vector (bottom plus lateral) appearing in Eq. (1). As shown by the solid line in Figure 9 the friction is relatively small along the eastern and northern boundaries. It is enhanced along the western ($800km < s < 1350km$) and southern ($1350km < s < 1750km$) boundaries in the northern marginal sea. The integral of the frictional stress around the entire *C*, *i.e.*, the left hand side of Eq. (2), is $1.54 \times 10^{-1}\ m^2s^{-2}$. The net transport of planetary vorticity (or volume flux of PV) across *C*, *i.e.*, the right-side term of Eq. (2), is $1.75 \times 10^{-1}\ m^2s^{-2}$, which is about 13% greater than the integral of frictional stress ($1.54 \times 10^{-1}\ m^2s^{-2}$). The difference is due to advection of the relative vorticity and time varying terms, all of which are assumed to be small in the derivation of Eq. (2). Overall, the integral balance (2) is reasonably well satisfied in the model and the prediction of overall anticyclonic flow, which follows from (4), is also successful.

The next idealized experiment ('*IDL*-2') explores a case in which dense water is fed into the interior through a passage that is deeper than the draining strait. In particular, the water-mass is specified as an inflow through a northern strait, analogous to the Fram Strait. Equation (5) may now be used, with Q_{FBC}=0 and H_{FS}<H_{int}, so that anticyclonic circulation around *C* is again predicted. Figure 7c shows that the inflow forms a cyclonic current along the northern and western boundaries. It is an analog of the East Greenland Current. The southward western boundary current, instead of continuing southward toward the sill, turns eastward, makes a U-turn, and approaches the strait as a westward coastal current along the model's `Iceland' toward the connecting strait. Since there is little flow along the northern and eastern boundaries, the anticyclonic 'NIJ' current must be sufficiently strong to overcome the cyclonic contribution from the model East Greenland Current. The flow pattern is essentially the same as that shown by Helfrich and Pratt (2003, their Figure 7a) and by Yang and Price (2000, their Figure 8a). It is also similar to that in EXP-3 with realistic bathymetry and a localized source on the Greenland slope (Figure 5a). The cumulative integral of bottom friction (dashed line in Figure 9) shows little contribution from the eastern boundary, a negative contribution from the northern and western boundaries, and a stronger positive contribution from the southern boundary or 'Iceland coast': 1350-1750km. It is interesting to note that the detachment from the southward WBC to form a westward flow along the northern coast of `Iceland' is also qualitatively similar to the separated EGC pathway described by Våge et al. (2013). However, their proposed detachment mechanism involves changes in the wind field along the Greenland coast, whereas detachment in the present, wind-free simulation is due to the topographic effect discussed by Helfrich and Pratt (2003) and Yang and Price (2000).

The integral of the circulation, as shown in (5), can be reversed if the source water enters the northern basin with a high PV. This can be accomplished by simply making the sill depth at the northern channel, *i.e.*, HFS in (5), shallower than that at the connecting channel. In the next experiment, we repeated IDL-2 with a small modification in bathymetry. The sill depth is set at 750m at the northern open boundary (Figure 8a). This localized change in bathymetry makes the right hand side term of (5) to be negative, a reverse from that in IDL-2. The integral of the circulation around C is cyclonic. The NIJ-like current vanishes (Figure 8b). In fact, the western boundary current, the model's EGC, continues southward and approaches the sill as a western boundary current. No detachment occurs.

As an integral constraint, Eq. (2), or its approximation (4), governs the total circulation around *C* but does not dictate the direction of flow along any subsegment. In fact, the flow along the western boundary in the second idealized experiment (*IDL-2*, Figure 7c) is actually southward or cyclonic. There are scenarios, including one discussed below, in which simulated flows satisfy (4) but lack NIJ-like currents. The assumption that the source water is formed in a deep basin and thus has a low PV is rather *ad hoc* and overly constraining. It is possible that a portion of the DSO source water is formed on the shallow shelf along the boundary and outside the contour *C*. So the integral constraint (4) or (5) is suggestive but not definitive. A stronger constraint is discussed next in Sec. 4.3 below, but first we consider the case in which the dense outflow is fed from shallow, coastal areas.

4.2. Net Sinking Near the Boundary.

Modeling work and observations over the past two decades (e.g. Böning et al. 1996; Marotzke and Shott 1999; Spall 2003, 2004; Pedlosky 2003; Straneo 2006; Våge et al. 2011; Cenedese 2012) suggests that deep convection in the interior of a high-latitude basin produces little net sinking, and that the later tends to occur close to boundaries. A cartoon expressing some of the elements of this work (in particular, Spall 2003 and 2004, Våge 2011 and Cenedese 2012) appears in Figure 10. A warm surface boundary current enters the marginal sea along the right-hand coast. This current could be analogous the North Icelandic Irminger Current, in which case the right-hand coast would correspond to the north coast of Iceland. The current is baroclinically unstable and sheds warm eddies that disperse into the interior, where they are cooled. This interior region experiences thermal convection down to some level but the spatially averaged vertical velocity is zero. So there is no net sinking, and thus the deep outflow is not fed from the interior. Instead there is a return flow of cooler eddies into the boundary current. Net sinking preferentially occurs in these models near the boundary itself, where the vorticity production by sinking-induced stretching is balanced by frictional effects. This mechanism also occurs in laminar models (e.g. Pedlosky 2003), but eddies are implicit in the parameterizations of friction and diffusion. The implication is that the cold outflow from the marginal sea is fed strictly by the boundary sinking, though this pathway has not been explicitly identified in any model. (Though interior convection is primarily an overturning process, a small net vertical velocity over a large area could also contribute to the outflow. Only one such study, that of Pratt and Spall (2008), considers a case where the marginal sea outflow is hydraulically controlled and partially blocked below sill depth, but the distribution of sinking and the source of the outflow was not determined.)

In light of the work just cited, we must also consider the possibility that the overflow is fed by sinking processes occurring near the boundary, perhaps entirely outside the contour C. We therefore explore a case in which w_e is finite only near the coast. In interpreting the results that follow, the reader may wish to keep in mind that the cross-interface velocity is associated with both sinking *and* water mass transformation in a layer model. The spatial separation between *thermodynamic* transformations and vorticity-producing net sinking that is possible in the continuously stratified models is difficult in the 2-layer formulation. The dynamical and thermodynamical consequences of w_e occur together, and when we specify sinking near a coast, the implication is that the water mass transformation also occurs there.

Some of the elements of coastal sinking were present in EXP-2, where a uniform w_e is initially applied in the whole Nordic Seas. As the flow evolves, the interface rises in the interior and the lower layer eventually outcrops over the deeper portions of the basin. The downwelling w_e in the outcropped region (within the black contour in Figure 4a) is then turned off and subsequently restricted to the region between the black line and the coast. Interpretation of the integral constraints (4) or (5) is tricky because w_e occurs both inside and outside C and thus the direction of Q_{int} is uncertain.

Because of this ambiguity, we conducted an additional experiment in which w_e is finite only outside of C. In the 4th experiment (EXP-4), a uniform downwelling w_e is applied only in areas where the depth is shallower than the DS sill depth (620m), areas within the purple contours in Figure 5b. In the deeper region inside of C, the downwelling w_e is set to zero. As shown in Figure 5b, the NIJ-like current remains a robust feature along the north coast of Iceland (Figure 5b). The PV integral is clearly not helpful in this case and we therefore seek a stronger constraint or mechanism that promotes the NIJ's existence.

4.3. Mechanism Two: An Island Circulation Integral Constraint

Here we consider the circulation integral around the contour C_I corresponding to a closed isobath lying slightly *above* the DS sill depth (620m) and circling the Iceland-Faroe ridge (Figure 6). This contour exists only when the marginal sea has two outlets. It passes unimpeded through the deeper Faroe Bank Channel (sill depth 840m) and lies well within the observed depth range of the NIJ.

We continue to assume that the Rossby number is small (so that $\zeta_2 << f$), that $|\eta_2| << h_2$, and that f is constant. (Although the Rossby number may not be small where C_I passes through the DS or FBC, the flux of ζ_2 across those segments may still be small.) Application of the circulation integral (2) around this contour leads to

$$\frac{fQ_I}{H_I} = \oint_{C_I} \vec{F}_2 \cdot \vec{l}\, ds \,, \qquad (7)$$

where H_I is the lower layer thickness around C_I and Q_i is the outward volume flux. The latter will be zero if the overflows are fed from regions of the basin lying offshore of C_I, in which case

$$\oint_{C_I} \vec{F}_2 \cdot \vec{l}\, ds = 0 \qquad (8)$$

Clearly, the shallower or closer to the Iceland coast that we choose C_I, the smaller Q_I is likely to be, but we do not want to choose an isobath that is shallower than the depth of the NIJ.

Our model uses a quadratic bottom drag $\vec{F} \; \square\square\!/\,|\vec{u}_2|\,\vec{u}_2/h_2$ so that Eq. (8) becomes:

$$\square\!/\!\oint_{C_I}(|\vec{u}_2|/h_2)\vec{u}_2 \,\square\, \vec{l}ds \;\square\, 0, \qquad (9)$$

so that the flow around C_I cannot be unidirectional. It must include segments of both cyclonic and anti-cyclonic circulation. A similar conclusion follows from the use of a linear bottom drag $\vec{F}_2 \; \square\square\!/\,\vec{u}_2$. Noting that the Faroe Bank Channel overflow tends to turn to the west as it enters the Atlantic Ocean and follows the southern slope of the Iceland-Faroe Ridge, it might be expected that the resulting anticyclonic contribution to the integral in (9) would require a balancing cyclonic (westward) flow (*i.e.*, the NIJ) along the north coast of the Ridge. This scenario is illustrated in the lower right inset of Figure 6.

We have tested these ideas by performing two additional idealized experiments. In both, we modify the Figure 7 model bathymetry by adding an additional strait, analogous to the Faroe Bank Channel, so that there is a closed geostrophic contour between two outflow channels (Figure 11). In the first of the new experiments (‘*IDL*-3’, Figures 11a,b), a water-mass source is introduced as an inflow through a northern inlet, and an outflow is placed on the southern boundary, just as that in *IDL-2* (Figure 7c). The water mass must exit through one or both straits from the northern to the southern basin, but the draining pathways are determined by the model dynamics.

Figure 11b shows the layer interface height and lower layer velocity at the end of a 10-year model run. In the upstream (northern) basin, the water mass enters the model domain and flows cyclonically along the northern and western boundary toward the western strait, the model's Denmark Strait. As in the 2nd idealized experiment (*IDL-2*, Figure 7c), the southward western boundary current (model's EGC) turns eastward into the interior instead of continuing southward toward the western strait. On the eastern side of the basin, there is a southward eastern boundary current that flows directly into the eastern strait, or the model's Faroe Bank Channel. As in Figure 7c, the overflow through the western strait is fed largely by an NIJ-like current along the north coast of the model's Iceland. Note the westward flow along the south coast of Iceland, originating from the model Faroe Bank Channel. The frictional stress associated with this flow is balanced in eq. (9) by that due to the NIJ. In general the flow is very similar to that in the IDL-2 (Figure 7c). The model NIJ can also be motivated in terms of the basin integral (5), without using the island integral (9), so we next present an experiment designed to distinguish between the consequences of the two constraints.

In the 4th idealized experiment (*IDL-4*), a shallow ridge is inserted between the southern boundary and the mid-basin island (Figure 11c). The northern basin is unchanged so that the application of the PV-integral about the northern basin is not affected. The insertion of this ridge, however, means that the island contour C_I is no longer closed and so Eq. (9) is no longer valid. Figure 11d shows the model flow at the end of a 10-year run. The circulation is similar to the previous run (Figure 11b) except that the NIJ vanishes completely. The overflow is mainly through the eastern strait or the model's FBC. The transport through the western strait (or the DS) is weak. In reality, there is a ridge (the Reykjanes Ridge) that runs southwest of Iceland, but the closed 620m contour crosses this feature. It is diverted to the southwest as it crosses, but it is not completely impeded as in IDL-4.

5. Wind-Stress Forcing

We have examined two mechanisms, *i.e.*, the basin circulation integral (4) and the around island integral (9), that promote the existence of the NIJ in source- and sink-driven overflows without wind-stress forcing. Wind-driven flows contribute to the DSO and wind stress is a main mechanism for transport variations in both Denmark Strait and Faroe Bank Channel (e.g., Biastoch et al., 2003; Köhl, et al., 2007; Nilsen et al., 2003; Serra et al., 2010). The role of wind-stress forcing in the existence of the NIJ is examined in this section. We use annual-mean wind stress climatology from the OAFlux (Yu et al., 2008). It represents an average between 1988 and 2008 with a resolution of 0.25^{o} degree. It is linearly interpolated to the model grids. In the first wind-driven experiment (*WIND-1*) the diapycnal water-mass flux term w_e is turned off and the model is forced solely by the surface wind stress from an initial state of rest with the layer interface set at 500m below sea surface. The circulations in both layers at the end of 5th year are shown in Figure 12. The flows in both upper- and lower-layers in the Nordic Seas are dominated by basin-wide cyclonic gyres. They are driven by positive curl of wind stress in the subpolar North Atlantic Ocean. The transport over the GISR is near zero in the lower layer since there are no water-mass sources or sinks in either basin.

There are several notable features in the lower-layer flows. First, the flow is always eastward on the north side of the Iceland-Faroe Ridge between the DS and FBC (Figure 12b). In all source/sink-driven experiments, however, the flow is always westward (Figure 3-5). The observed situation is apparently more complex than either of the above. Between the DS and Jan Mayen Ridge the flow is the westward NIJ. But to the east of the Jan Mayen Ridge, the flow is eastward according to Søiland et al. (2008) who used neutrally buoyant floats to trace the flow pathway. This current is the main pathway for the Faroe Bank Channel Overflow (Søiland et al., 2008). None of the experiments described so far are able to simulate these two opposite currents. The flow is in the wrong direction between DS and Jan Mayen Ridge in the wind-driven run (Figure 12) and between the Faroe Islands and Jan Mayen Ridge in source/sink-driven experiments (Figure 3-5). This suggests that both wind stress and buoyancy forcing could be important for the Nordic Seas Overflow pathways. To explore this further we add wind stress forcing to the previous experiment with a uniform w_e (EXP-2W). The flow in the lower layer is shown in Figure 13. The circulation changes significantly when the wind stress is added. The two opposite currents along the northern Iceland-Faroe Shelf/Slope are simulated in EXP-2W with a uniform w_e (Figure 13). The eastward flow along Iceland-Faroe Ridge appears to be a continuation from a southward transport along the Jan Mayen Ridge. This pathway for the Faroe Bank Channel Overflow is consistent with observations described by Søiland et al. (2008). The eastward jet along Iceland-Faroe Ridge also emerges in other source-/sink-driven experiments when wind-stress is added (not shown). Along the continental shelf north of Iceland, the addition of wind-stress forcing in the model weakens but does not eliminate (at least for the climatological mean wind stress) the NIJ. The model NIJ extends far less eastward when compared with Figure 4a. In fact, the westward flow along northeastern coast of Iceland begins around 14-15W, which is roughly consistent with the observations by Våge et al. (2013). The NIJ transport appears to be supplied by a cyclonic gyre in the Iceland Sea and a small anti-cyclonic gyre between Jan Mayen Ridge and Iceland to the south of the Iceland Sea (Figure 13).

A second notable feature of the wind-only experiment is that the EGC pathway becomes more prominent (Figure 12) in both layers. The EGC is weak south of the Greenland Sea in the dam-break and the source/sink-driven experiments (Figures 3-4). It is strengthened as the western boundary current of the wind-driven cyclonic gyre in the Nordic Seas (Figure 13). This would support previous modeling studies (e.g. Köhl, 2010) suggesting that a strong wind-stress forcing, such as during a high North Atlantic Oscillation state, enhances the EGC transport and weakens the NIJ pathway. It is interesting to note that there are three branches of the DSO, the EGC, the NIJ and S-EGC, when wind stress is added. Without the wind stress, both the EGC and S-EGC are basically absent (Figure 4b). So the wind stress is essential for the existence of both the EGC and S-EGC in the model even though the formation of the S-EGC is mainly due to topographic effect.

Finally, we note that the deep circulations in Greenland Sea, Norwegian Sea, Iceland Sea and Lofoten Basin become cyclonic when wind stress is added. They are mostly anti-cyclonic in previous source/sink-driven experiments (EXP-1, 2 and 3) without wind-stress forcing. The eastern boundary current along Norway's coast becomes northward in this wind-driven model runs. The flow along the mid-ocean ridge, Jan Mayen and Mohn Ridges, is southward toward the GISR, which consistent with what was found by Søiland et al. (2008). In the source/sink-driven flows, the flow is northward along the mid-ocean ridge. In most cases with wind stress forcing discussed here the lower layer outcrops in the Nordic Seas and thus is exposed to wind stress forcing. This direct wind-stress forcing contributes to circulation changes in the lower layer.

The wind stress forces a cyclonic boundary current that is opposite to the NIJ along the north coast of Iceland. Figure 13 shows that the climatological wind stress in the model is not strong enough to reverse the NIJ. But one would wonder how resilient the NIJ is to an abnormally strong wind-stress forcing, either due to a seasonal cycle or to atmospheric variability. We conducted two additional experiments (not shown here), one with wind stress increased by a factor of 2 and the other by factor of 5. The westward NIJ is still present even when the climatological wind stress is doubled. But the flow along the north Icelandic coast changes to eastward when the wind stress is increased by a factor of 5.

6: Summary

A two-layer model is used to examine mechanisms that encourage the existence of the North Icelandic Jet – ostensibly a major pathway for the Denmark Strait Overflow. This study identifies and tests two integral constraints that bear on the existence of the NIJ. The first is a circulation integral around a closed contour *C* that circles those central portions of the upstream basin for which the depth is greater than the sill depth. An outward flow from these deeper regions implies a net divergence in the lateral PV transport in the deep Nordic Basin, which implies an anticyclonic acceleration of the circulation around *C*. In a steady state this tendency must be balanced by a cyclonic frictional torque and implies anti-cyclonic flow around *C*. A westward NIJ is consistent with this picture, though not required, and the need for such a flow is strengthened by the presence of the (cyclonic) EGC. A similar result is obtained when the overflow is fed by a deep source whose thickness exceeds that of the overflow. Although both cases are suggestive, we also find a westward NIJ when sinking occurs mainly in the shallower regions outside of *C*. In this case the circulation integral around *C* is uninformative. The second, stronger constraint is contained in the circulation integral around a closed geostrophic contour C_I that lies slightly above the sill depth of the Denmark Strait and circles around Iceland and the Iceland-Faroe Ridge, passing unimpeded through the deeper Faroe-Bank Channel. If there is no wind and no net exchange between the upper and lower layers inside C_I the circulation around C_I is zero and so the tangential component of the velocity about it cannot be unidirectional. The FBC overflow produces a predominantly anti-cyclonic tangential velocity along the eastern and southern segments of C_I, and an NIJ-like western flow along the segment north of Iceland would tend to balance this.

A positive wind stress curl forces cyclonic circulations in both layers. The basin-wide circulation, including flows along the mid-ocean ridges, is strongly affected by wind stress. The wind-driven surface flow along the north Icelandic shelf is eastward and against the NIJ. The wind weakens but does not eliminate the NIJ and it produces a more realistic eastward flow in the lower layer to the east of the Jan Mayen Ridge. The presence of the wind also produces cyclonic flow in the Lofoten, Norwegian and Greenland Basins, which is in general agreement with observations. The wind stress also promotes the EGC pathway, and it is postulated that the NIJ pathway would be more dominant when wind stress forcing is weak, such as during a low state of the North Atlantic Oscillation, while the EGC becomes more important when wind is strong.

A reviewer has asked us to comment on the fact that net downwelling can become smaller over time due to the outcropping of the lower layer. In our runs, where the initial upper layer thickness is hundreds of meters, outcropping occurs in about 2 years, whereas the steady state solutions that we actually analyze are examined after 10 years or so. So the pre-outcropping phase is quite short compared to the total run time. Accordingly, we have not attempted to analyze transients and other adjustment features that are triggered when outcropping occurs and the total downwelling decreases. This is an interesting problem, however, and perhaps one of the keys to variability of the Nordic Seas outflows. It is beyond the scope of the current paper, but a good problem for future study.

Acknowledgement:

This study has been supported by National Science Foundation (OCE0927017, ARC1107412). We thank Drs. Femke de Jong, Bob Pickart, Mike Spall and two thorough reviewers for their comments and suggestions.

References:

Aagaard, K., Fahrbach, E., Meincke, J., and Swift, J. H. 1991: Saline outflow from the Arctic Ocean: Its contribution to the deep waters of the Greenland, Norwegian and Icelandic seas. *J. Geophys. Res*., **96**: 20433–20441.

Biastoch, A., R. H. Käse and D. B. Stammer, 2003: The sensitivity of the Greenland-Scotland Ridge Overflow to forcing changes. *J. Phys. Oceanogr.*, **33**, 2307-2319.

Buch, E., Malmberg, S.-A., and Kristmannsson, S. S. 1996: Arctic Ocean deep water masses in the western Iceland Sea. *J. Geophys. Res*., **101**: 11965–11973.

Böning, C. W., F. O. Bryan, W. R. Holland and R. Doescher, 1996. Deep-water formation and meridional overturning in a high-resolution model of the North Atlantic. *J. Phys. Oceanogr*. **26**, 1142-1164.

Cenedese, C. 2012. Downwelling in Basins Subject to Buoyancy Loss. *J. Phys. Oceanogr*. **42**, 1817-1833.

Dickson, R., S. Dye, S. Jonsson, A. Kohl, A. Macrander, M. Marnela, J. Meincke, S. Olson, B. Rudels, H. Valdimarsson and G. Voet, 2008: The overflow flux west of Iceland: variability, origins and forcing. In *Arctic-Subarctic Ocean Flux*, edited by R. R. Dickson, J. Meincke and P. Rhines, page 443-474, Springer, pp736.

Dickson, R.R., Brown, J., 1994. The production of North Atlantic Deep Water, Sources, rates, and pathways. J*ournal of Geophysical Research*, **99**, 12319–12341.

Eldevik, T., Nilsen, J.E.Ø., Iovino, D., Olsson, K.A., Sandø, A.B. and H. Drange, 2009: Observed sources and variability of Nordic Seas overflow. Nat. Geosci. 2, 406–410.

Girton, J. B., and T. B. Sanford, 2003: Descent and modification of the overflow plume in the Denmark Strait, *J. Phys. Oceanogr*., 1351-1364.

Girton, J. B., T. B. Sanford, and R. H. Käse, 2001: Synoptic sections of the Denmark Strait overflow, *Geophys. Res. Lett*., 28, 1619– 1622.

Hansen, B. and S. Østerhus, 2000: North Atlantic-Nordic Seas exchanges. *Prog. Oceanogr*., 45, 109-208.

Hansen, B. and S. Østerhus, 2007: Faroe Bank Channel overflow 1995-2005. Progress in Oceanography, Vol 75, 817-856.

Hansen, B., S. Østerhus, W. R. Turrell, S. Jonsson, H. Valdimarsson, H. Hatun and S. M. Olsen, 2008: The inflow of Atlantic water, heat and salt to the Nordic Seas across the Greenland-Scotland Ridge. Page 15-43, in *Arctic-Subarctic Ocean Flux*, edited by R. R. Dickson, J. meincke and P. Rhines. Springer, pp 736.

Helfrich, K. R. and L. J. Pratt, 2003: Rotating hydraulics and the upstream basin circulation. *J. Phys. Oceanogr*., **33**, 1651-1663.

Isachsen, P. E., C. Mauritzen and H. Svendsen, 2007: Dense water formation in the Nordic Seas diagnosed from sea surface buoyancy fluxes. *Deep Sea. Res*., **54**, 22-41.

Jeansson, E., S. Jutterström, B. Rudels, L. G. Anderson, K. A. Olsson, E. P. Jones, W. M. Smethie Jr. and J. H. Swift, 2008: Sources to the East Greenland Current and its contribution to the Denmark Strait Overflow. *Progress in Oceanography*, **78**, 12-28.

Jónsson, S., 1999. The circulation in the northern part of the Denmark Strait and variability. ICES CM, 9.

Jónsson, S. and Valdimarsson, H. 2004, A new path for the Denmark Strait overflow water from the Iceland Sea to Denmark Strait. *Geophys. Res. Lett*., 31, L03305.

Karcher, M., F. Kauker, R. Gerdes, E. Hunke, and J. Zhang, 2007: On the dynamics of Atlantic Water circulation in the Arctic Ocean, *J. Geophys. Res*., 112, C04S02, doi:10.1029/2006JC003630.

Karcher, M., R. Gerdes and F. Kauker, 2008: Long-term variability of Atlantic water inflow to the Northern Seas: Insights from model experiments. page 111-130, in *Arctic-Subarctic Ocean Flux*, edited by R. R. Dickson, J. meincke and P. Rhines. Springer, pp 736.

Käse, R. H., J. B. Girton and T. B. Sanford, 2003: Structure and variability of the Denmark Strait Overflow: Model and observations. *J. Geophys. Res.*, **108,** 3181, doi:10.1029/ 2002JC001548,

Käse, R. H. 2006: A Riccati model for Denmark Strait overflow variability. *Geophys. Res. Lett.*, Vol 33, L21S09, doi:10.1029/2006GL026915.

Käse, R. H., N. Serra, A. Köhl and D. Stammer, 2009: Mechanisms for the variability of dense water pathways in the Nordic Seas. *J. Geophys. Res*., Vol 114, C01012, doi:10.1029/2008JC004916.

Köhl, A, 2010: Variable source regions of Denmark Strait and Faroe Bank Channel, *Tellus*, **62A**, 551-568.

Köhl, A, R. H. Käse, D. Stammer and N. Serra, 2007: Causes of changes in the Denmark Strait Overflow. J. Phys. Oceanogr., 37., 1678-1696.

Lake, I., K. Borenas and P. Lundberg, 2005: Potential-vorticity characteristics of the Faroe Bank Channel deep-water overflow. *J. Phys. Oceanogr.*, **35**, 921-931.

Macrander A, Send U, Valdimarsson H, Jónsson S, Käse RH, 2005: Interannual changes in the overflow from the Nordic Seas into the Atlantic Ocean through Denmark Strait. *Geophys Res Lett*, 32:L06606, DOI 10.1029/2004GL021463.

Macrander, A., R. H. Käse, U. Send, H. Valdimarsson, S. Jonsson, 2007: Spatial and temporal structure of the Denmark Strait Overflow by acoustic observations. *Ocean Dynamics*, **57**, 75-89.

Marotzke, J. and J. R. Schott 1999. Convective mixing and the thermohaline circulation. *J. Phys. Oceanogr*. **29**, 2962-2970.

Mauritzen, C. 1996a: Production of dense overflow waters feeding the North Atlantic across the Greenland-Scotland Ridge. 1. Evidence for a revised circulation scheme. Deep Sea Res. I 43, 769–806.

Mauritzen, C. 1996b: Production of dense overflow waters feeding the North Atlantic across the Greenland Sea-Scotland Ridge. Part 2: An inverse model. *Deep-Sea Research*, **43**: 807–835.

Nilsen, J. E. Ø., Y. Gao, H. Drange, T. Furevik, and M. Bentsen, 2003: Simulated North Atlantic-Nordic Seas water mass exchanges in an isopycnic coordinate OGCM, *Geophys. Res. Lett*., **30(10)**, 1536, doi:10.1029/2002GL016597.

Olsen, S. M., B. Hansen, D. Quadfasel and S. Østerhus, 2008: Observed and modeled stability of overflow across the Greenland-Scotland ridge. *Nature*, Vol 455, doi:10.1038/nature07302.

Pedlosky, J., 2003. Thermally driven circulation in small ocean basins. *J. Phys. Oceanogr*. **33**, 2333-2340.

Pratt, L. J., 1997: Hydraulically drained flows in rotating basins. Part II: Steady flow. *J. Phys. Oceanogr.*, **27**(12), 2522-2535.

Pratt, L. J. and M. Spall, 2008. Circulation and exchange in choked marginal seas. *J. Phys. Oceanogr.*, **38**(12), 2639-2661.

Pratt, L. J., and J. Whitehead, 2008. *Rotating Hydraulics*, Springer (New York), 582pp.

Price, J. F., and M. O. Baringer, 1994. Outflows and deep water production by marginal seas. *Progress in Oceanography*, **33**, 161-200.

Rudels, B., E. Fahrbach, E. Meincke, G. Budeus, P. Eriksson, 2002: The east Greenland Current and its contribution to the Denmark Strait overflow. *ICES J.Mar. Sci*., **59**, 1133-1154.

Rudels, B., P. Eriksson, E. Buch, G., Budéus, E. Fahrbach and co-authors, 2003: Temporal switching between souces of the Denmark Strait overflow waters. *ICES Marine Sci. Symp.*, **219**, 319-325.

Serra, N., R. H. Käse, A. Kohl, D. Stammer and D. Quadfadsel, 2010: On the low-frequency phase relation between the Denmark Strait and the Faroe-Bank Channel overflows. *Tellus*, 62A, 530-550.

Smethie, W.M. and Swift, J.H. 1989. The tritium:krypton-85-age of Denmark Strait overflow water and the Gibbs Fracture Zone water just south of Denmark Strait. J. Geophys. Res. 94, 8265–8275.

Søiland, H., Prater, M.D. and Rossby, T. 2008. Rigid topographic control of currents in the Nordic Seas. Geophys. Res. Lett. 35, doi:10.1029/2008GL034846.

Spall, M. A. and Price, J. F., 1998. Mesoscale Variability in Denmark Strait: The PV Outflow Hypothesis, *J. Phys. Oceanogr*., **28**, 1598–1623, 1998.

Spall, M., 2003. On the thermohaline circulation in flat-bottom marginal seas. *J. Marine Res.*, **61**, 1-25.

Spall, M., 2004: Boundary currents and watermass transformation in marginal seas. J. Phys. Oceanogr., Vol 34, 1197-1213.

Spall, M., 2010: Non-local topographic influences on deep convection: An idealized model for the Nordic Seas. *Ocean Modeling*, Vol 32, 72-85.

Straneo, F. 2006. On the connection between dense water formation, overturning, and poleward heat transport in a convective basin. *J. Phys. Oceanogr.* **36**, 606-628.

Swift, J.H., Aagaard, K. and Malmberg, S. 1980: The contribution of Denmark Strait overflow to the deep North Atlantic. Deep Sea Res. 27, 29–42.

Tanhua, T., Olsson, K.A. and Jeansson, E. 2005: Formation of Denmark Strait overflow water and its hydro-chemical composition. J. Marine Syst. 57, 264–288.

Whitehead, J. A., A. Leetma, and R. A. Knox, 1974. Rotating hydraulics of strait and sill flows. Geophys. Fluid Dyn., 6, 101–125.

Våge, K., R. S. Pickart, M.A. Spall, H. Valdimarsson, S. Jonsson, D.J. Torres, S. Osterhus, T. Eldevik, 2011: Significant role of the North Icelandic Jet in the formation of Denmark Strait Overflow Water *Nature Geoscience,* ***4*** 723-727. doi:10.1038/ngeo1234

Våge, K., R. S. Pickart, M.A. Spall, G. W. K. Moore, H. Valdimarsson, D. J. Torres, S. Y. Erofeeva and J. E. Nilsen, 2013: Revised circulation scheme north of the Denmark Strait, *Deep-Sea Research*, **79**, 20-39.

Yang, J., and J. F. Price, 2000: Water mass formation and potential vorticity balance in an abyssal ocean circulation model. *J. Mar. Res.,* **58,** 789–808.

Yang, J, 2005: The Arctic and subarctic-ocean flux of potential vorticity and the Arctic Ocean circulation. *Journal of Physical Oceanography*, **35**, 2387-2407.

Yang, J. and J. F. Price, 2007: Potential-vorticity constraint on the flow between two basins. *Journal of Physical Oceanography*, **37**, 2251-2266.

Yang, J. and L. Pratt, 2013: On the effective capacity of the dense-water reservoir for the Nordic Seas overflow: some effects of topography and wind stress. *J. Physical Oceanogr*., 43, 418-431.

Yu, L., X. Jin, and R. A. Weller, 2008. Multidecade Global Flux Datasets from the Objectively Analyzed Air-sea Fluxes (OAFlux) Project: Latent and sensible heat fluxes, ocean evaporation, and related surface meteorological variables. Woods Hole Oceanographic Institution, OAFlux Project Technical Report. OA-2008-01, 64pp. Woods Hole. Massachusetts.

Figure Caption:

Figure 1: The model domain and bathymetry (meters). The East Greenland Current (EGC) has been considered as the main pathway for the DSO (Rudels, et al., 2002). But more recent observations showed that the North Icelandic Jet (NIJ) is another major pathway for the DS Overflow (Jonsson and Valdimarsson, 2004; Våge, et al., 2011). The separated EGC (S-EGC) is a branch of DSO that was discussed by Våge, et al. (2013). Note that the NIJ is a subsurface current while S-EGC is a surface current. The white-colored circle in the southwestern corner marks the area of upwelling from the lower to the upper layer,

Figure 2: (a) The initial condition for the dam-break experiment. The dense water in the Nordic Seas is set to be 50m below the sea surface. The lighter water fills the rest of the model domain. (b) A schematic north-south section of the initial condition.

Figure 3: (a) The sea surface height and depth-integrated velocity $h_1(u_1,v_1)$ in the upper layer, and (b) the depth-integrated velocity in the lower layer and bathymetry at the end of 1-year model run in the dam-break experiment (EXP-1).

Figure 4: Same as Figure 3 except for EXP-2. The downwelling w_e is uniform initially over the whole Nordic Seas within the red contour shown in the upper panel. The lower layer outcrops in the interior Nordic Seas at the end of the 10th year (within the black contour). The downwelling w_e is turned off whenever the lower layer outcrops. So the downwelling occurs only within the area between the red and black lines in the upper panel. The NIJ is robust and is a preferred pathway for the DSO.

Figure 5: (a) Lower-layer flow from EXP-3 in which w_e is located on Greenland Sea slope (within the purple contour). Despite the location of w_e in the EGC path, the NIJ emerges as the dominant DSO pathway. (b) Low-layer velocity in EXP-4. The water source w_e is located in areas (within purple contours) where the depth is shallower than the DS sill depth (620m). The PV integral constraint, Eq. (6) or (8), no longer favors the NIJ existence in this run. The existence of the NIJ indicates that there is likely another dynamical mechanism that promotes the existence of the NIJ.

Figure 6: The schematics of the integration paths for the two circulation constraints. The first integral, i.e., Eq. (5), is along the contour *C* in the central basin. The second integral, Eq. (8), is C_I around the Iceland-Faroe Ridge.

Figure 7: (a) Model bathymetry that is used in two idealized experiments (IDL-1 and 2); (b)the layer thickness anomaly and velocity from IDL-1, in which an open-ocean downwelling; and (c) the same as (b) except from IDL-2 except that the water-mass source is specified as an inflow at the northern boundary. The overflow approaches the sill as anti-cyclonic flow

in the northern basin, similar to the NIJ. These experiments are designed to demonstrate the first NIJ mechanism, i.e., the impact of PV modification on the upstream pathways.

Figure 8: Same as IDL-2 experiment as shown in Figure 7a&c except that the sill depth at the northern open channel is set to be 750m, which is shallower than 1250m - the sill depth of the connecting channel between two basins. This is equivalent to changing H_{FS} in Eq. (4) and (5). The right hand side of (5) becomes negative, the opposite to that in IDL-2. The circulation integral around C becomes cyclonic. The NIJ-like flow vanishes.

Figure 9: Integration of friction along the isobaths of 1500m in northern basin for IDL-1 (solid line) and IDL-2 (dashed line). The integration starts at the southeastern corner in the northern basin. The increase of the frictional torque is mainly induced by the NIJ-like currents along the southern boundary of the northern basin.

Figure 10: A cartoon that schematizes GCM results from the work of Spall (2003, 2004, and 2010). A warm surface boundary current enters the marginal sea along the right-hand coast. It is baroclinically unstable and sheds warm eddies that disperse into the interior, where they are cooled. The dense water is formed in the interior by convection but the spatially averaged vertical velocity is zero. So the deep outflow is not fed from the interior. There is a return flow of cooler eddies into the boundary current where net sinking preferentially occurs. The implication is that the cold outflow from the marginal sea is fed strictly by the boundary sinking.

Figure 11: Two idealized experiments (IDL-3 and 4) are designed to elucidate the circulation integral constraint on the existence of the NIJ. The NIJ exists in the IDL-3 (upper panels) because the there exists a closed geostrophic contour that encompasses the island. Along this contour there must be a cyclonic flow to counter the anti-cyclonic overflow through the eastern channel. In the lower panel (IDL-4), such a closed geostrophic contour no longer exists due to an insertion of a ridge in the southern basin. The integral constraint is no longer valid and the NIJ-like current disappears.

Figure 12: The sea surface height and surface velocity (top panel) and the bathymetry and lower-layer flow (bottom panel). The circulation in the lower layer is cyclonic in the whole Nordic Basin and in each sub-basin. The flow along the north Icelandic shelf and slope is eastward against the NIJ. This implies that wind stress forcing acts against the NIJ.

Figure 13: The same as Figure 4b except that the wind stress is applied. The circulation in the overflow layer changes significantly. The EGC pathway is elevated. The flow to the east of the Jan Mayen Ridge is now eastward along the Iceland-Faroe Ridge and becomes the main pathway for the FBC overflow. The flow along the mid-ocean ridges is southward toward the GISR. The circulations in the Nordic Seas are cyclonic. The most relevant feature is that the NIJ still exists robustly along the 600-1000m isobaths toward the Denmark Strait. So the NIJ is not eliminated by wind stress.

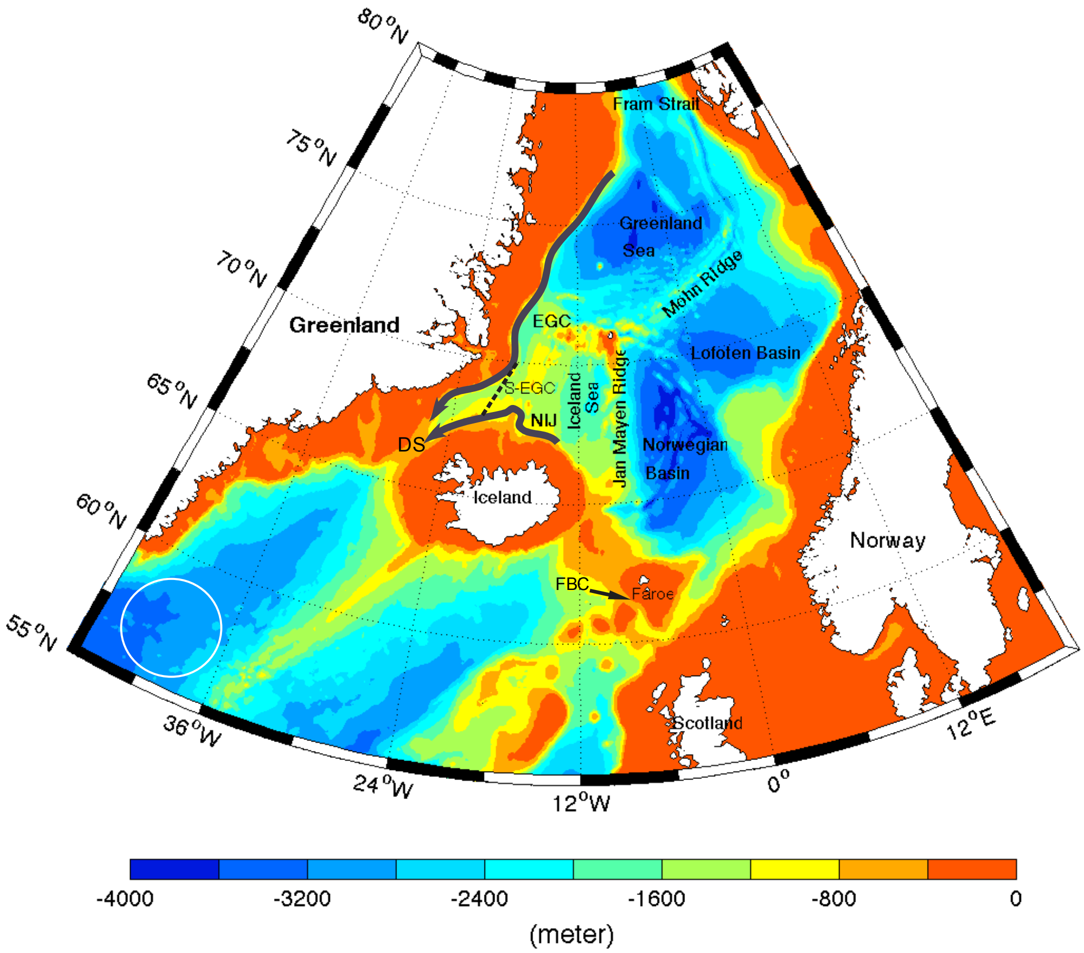

Figure 1: The model domain and bathymetry (meters). The East Greenland Current (EGC) has been considered as the main pathway for the DSO (Rudels, et al., 2002). But more recent observations showed that the North Icelandic Jet (NIJ) is another major pathway for the DS Overflow (Jonsson and Valdimarsson, 2004; Våge, et al., 2011). The separated EGC (S-EGC) is a branch of DSO that was discussed by Våge, et al. (2013). Note that the NIJ is a subsurface current while S-EGC is a surface current. The white-colored circle in the southwestern corner marks the area of upwelling from the lower to the upper layer,

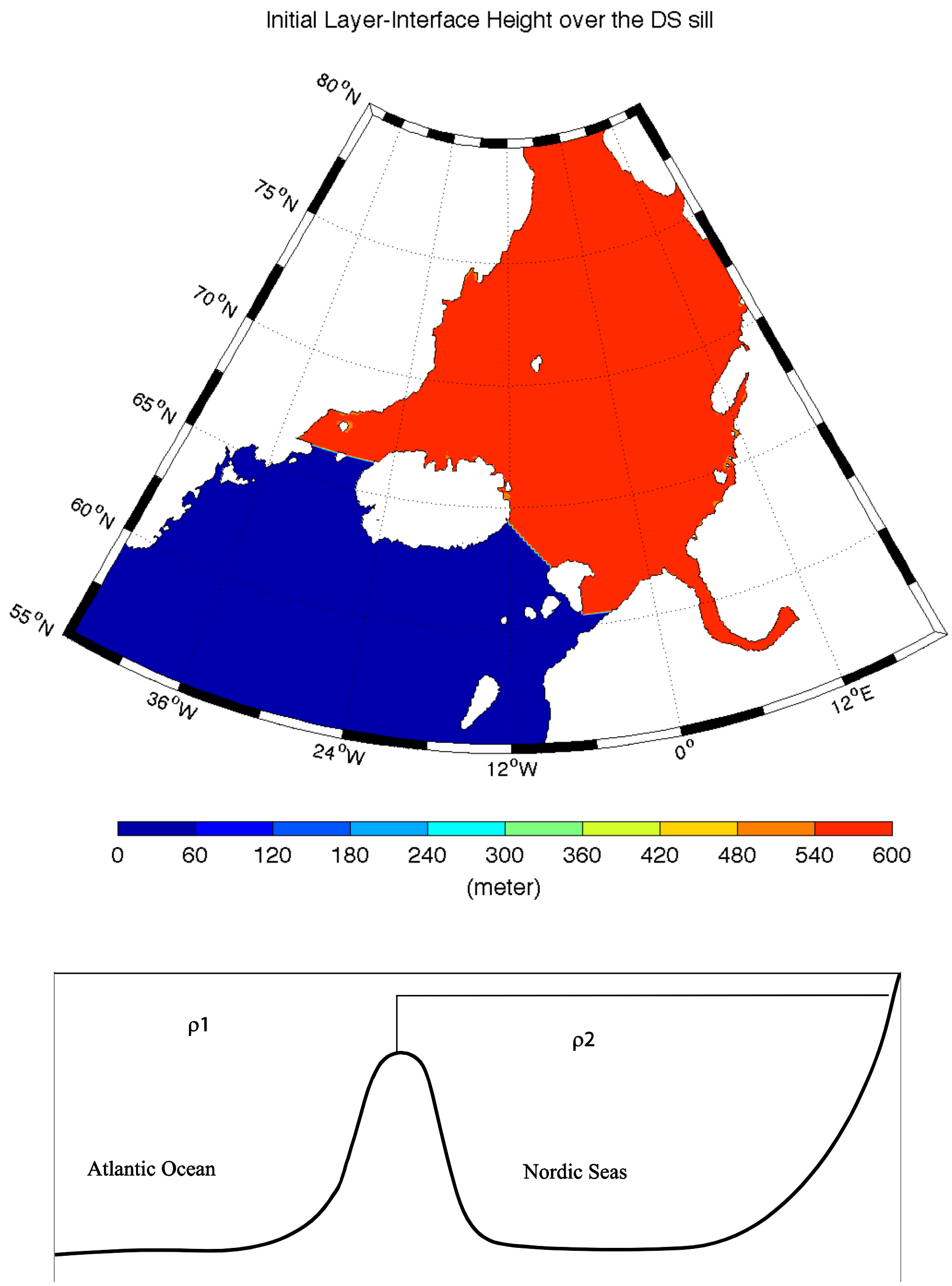

Figure 2: (a) The initial condition for the dam-break experiment. The dense water in the Nordic Seas is set to be 50m below the sea surface. The lighter water fills the rest of the model domain. (b) A schematic north-south section of the initial condition.

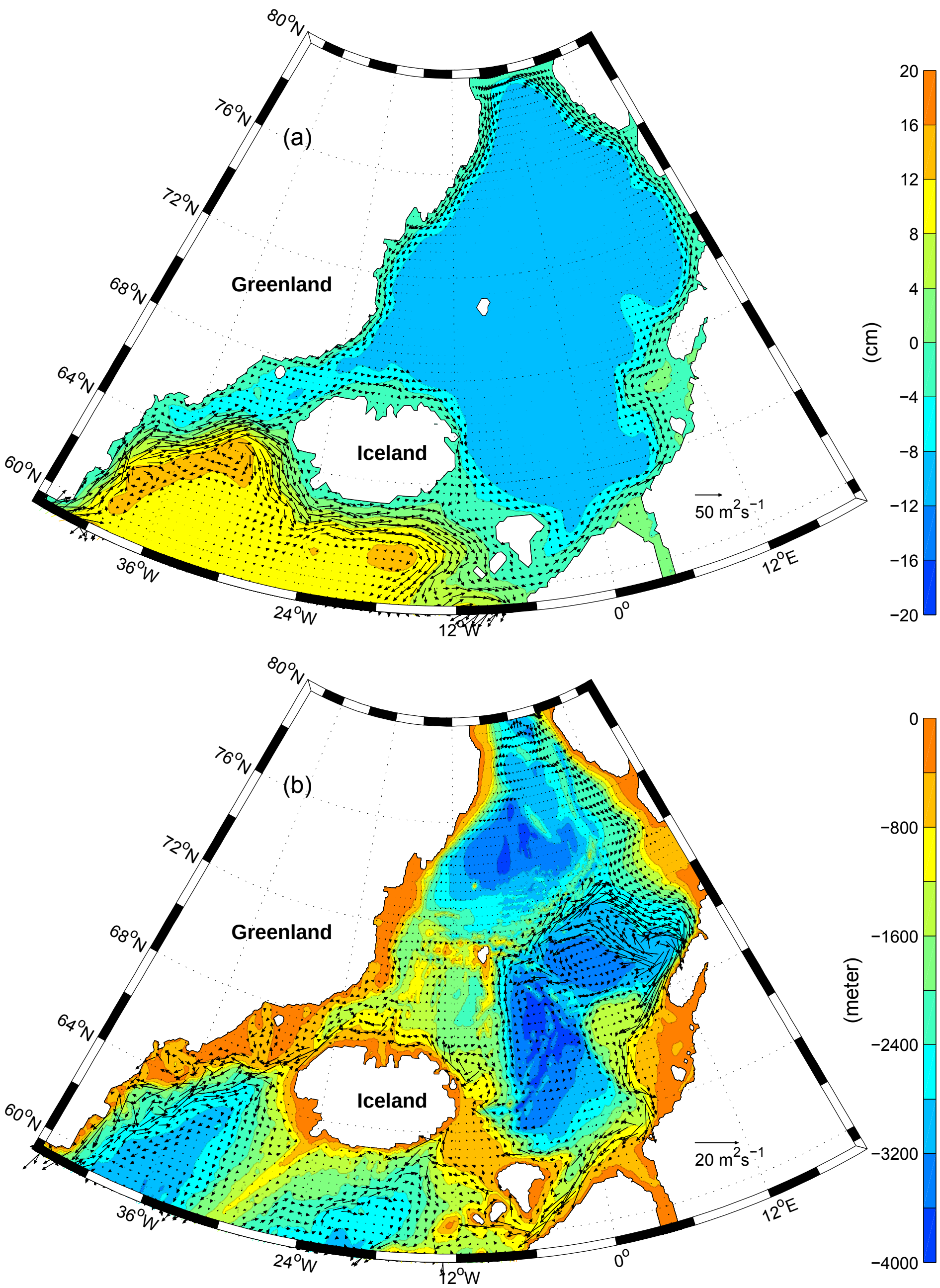

Figure 3: (a) The sea surface height and depth-integrated velocity $h_1(u_1,v_1)$ in the upper layer, and (b) the depth-integrated velocity in the lower layer and bathymetry at the end of 1-year model run in the dam-break experiment (EXP-1).

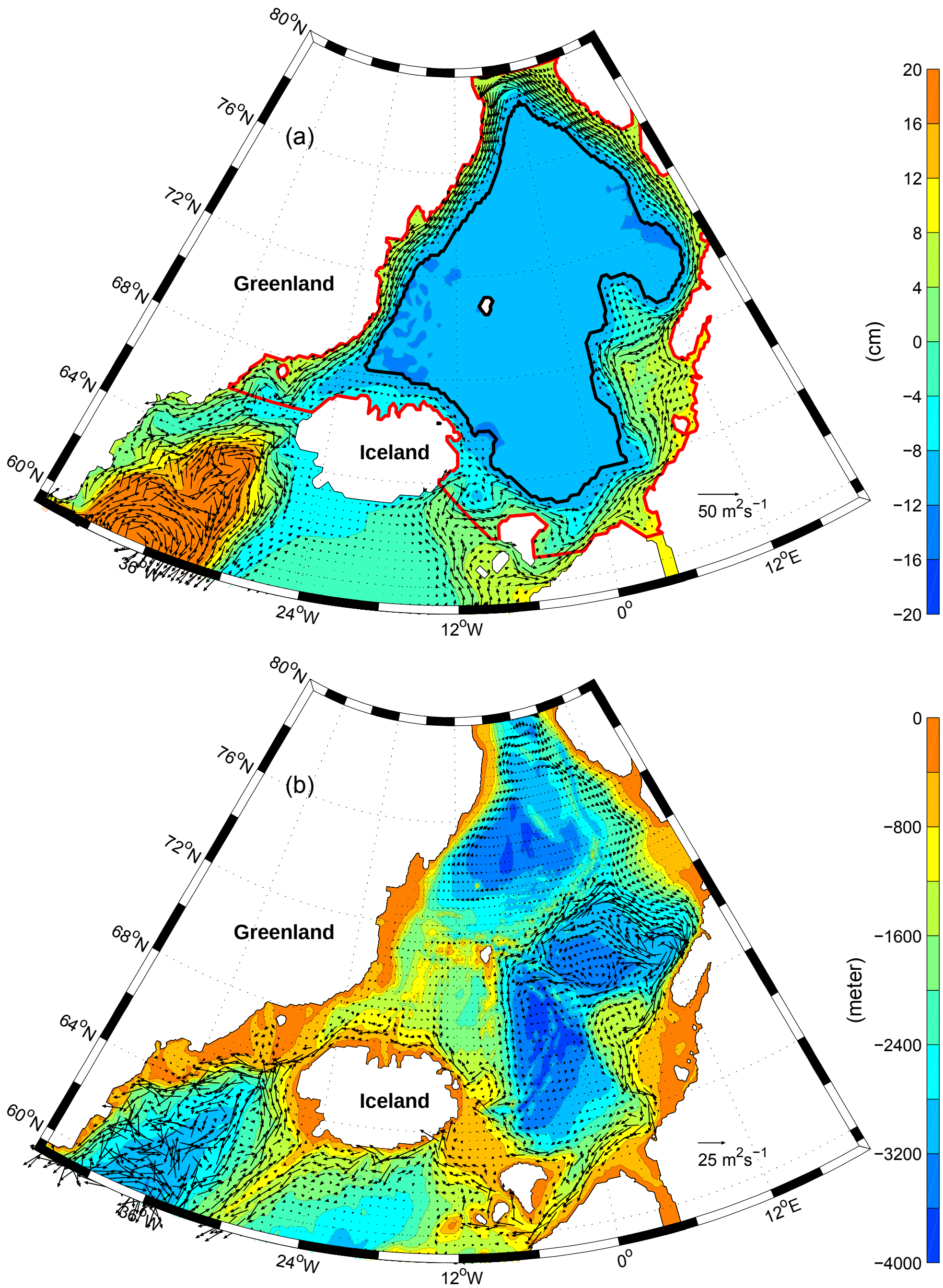

Figure 4: Same as Figure 3 except for EXP-2. The downwelling w_e is uniform initially over the whole Nordic Seas within the red contour shown in the upper panel. The lower layer outcrops in the interior Nordic Seas at the end of the 10th year (within the black contour). The downwelling w_e is turned off whenever the lower layer outcrops. So the downwelling occurs only within the area between the red and black lines in the upper panel. The NIJ is robust and is a preferred pathway for the DSO.

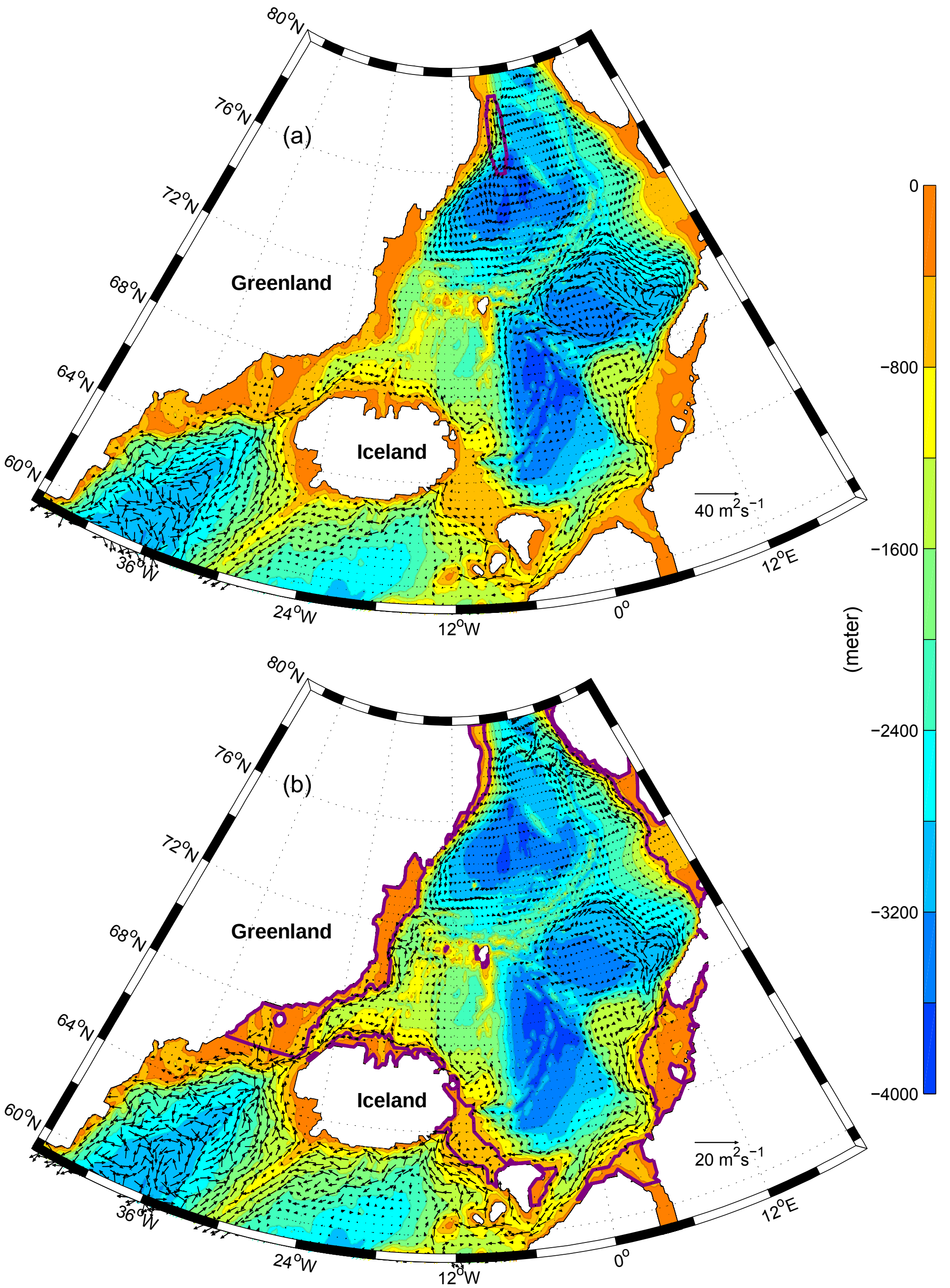

Figure 5: (a) Lower-layer flow from EXP-3 in which w_e is located on Greenland Sea slope (within the purple contour). Despite the location of w_e in the EGC path, the NIJ emerges as the dominant DSO pathway. (b) Low-layer velocity in EXP-4. The water source w_e is located in areas (within purple contours) where the depth is shallower than the DS sill depth (620m). The PV integral constraint, Eq. (6) or (8), no longer favors the NIJ existence in this run. The existence of the NIJ indicates that there is likely another dynamical mechanism that promotes the existence of the NIJ.

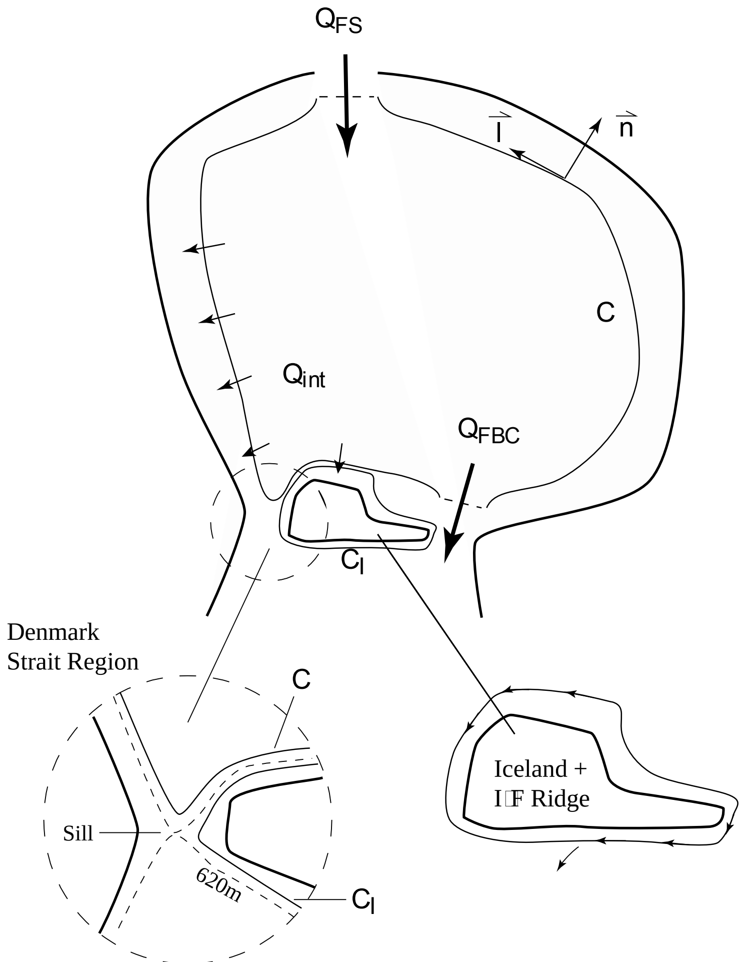

Figure 6: The schematics of the integration paths for the two circulation constraints. The first integral, i.e., Eq. (5), is along the contour C in the central basin. The second integral, Eq. (8), is C_I around the Iceland-Faroe Ridge.

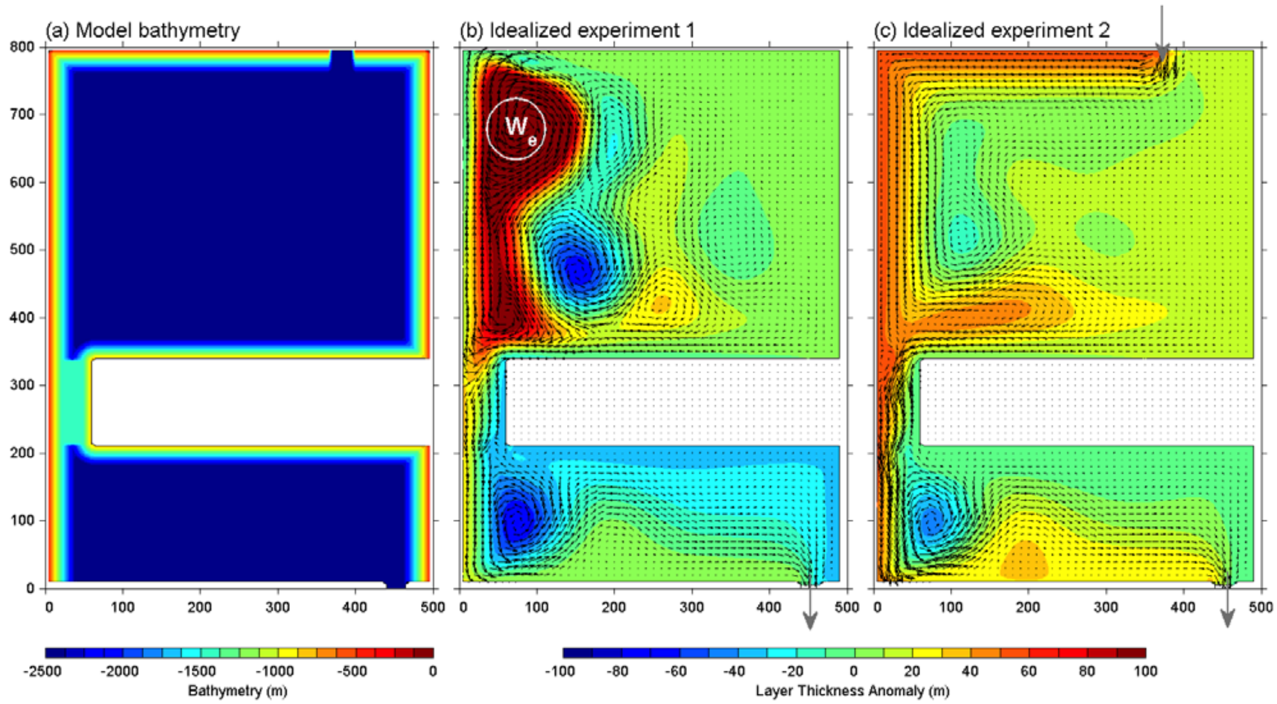

Figure 7: (a) Model bathymetry that is used in two idealized experiments (IDL-1 and 2); (b)the layer thickness anomaly and velocity from IDL-1, in which an open-ocean downwelling; and (c) the same as (b) except from IDL-2 except that the water-mass source is specified as an inflow at the northern boundary. The overflow approaches the sill as anti-cyclonic flow in the northern basin, similar to the NIJ. These experiments are designed to demonstrate the first NIJ mechanism, i.e., the impact of PV modification on the upstream pathways.

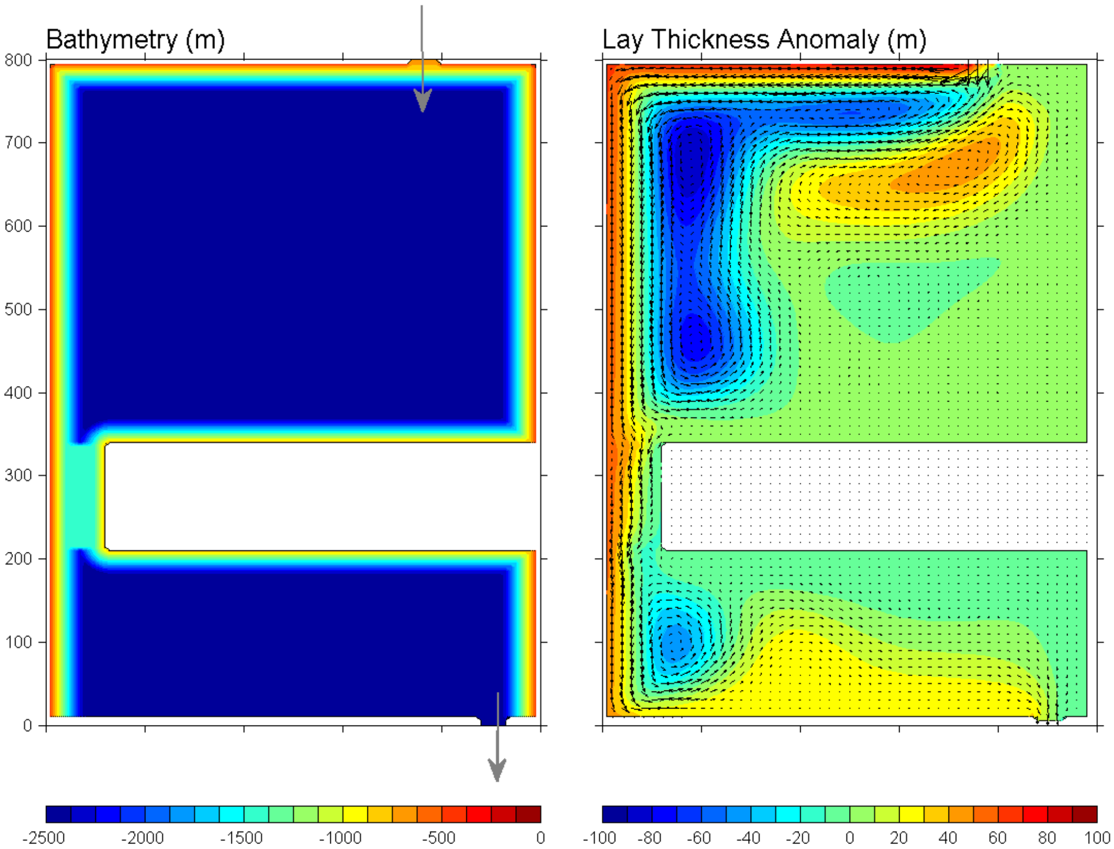

Figure 8: Same as IDL-2 experiment as shown in Figure 7a&c except that the sill depth at the northern open channel is set to be 750m, which is shallower than 1250m - the sill depth of the connecting channel between two basins. This is equivalent to changing H_{FS} in Eq. (4) and (5). The right hand side of (5) becomes negative, the opposite to that in IDL-2. The circulation integral around C becomes cyclonic. The NIJ-like flow vanishes.

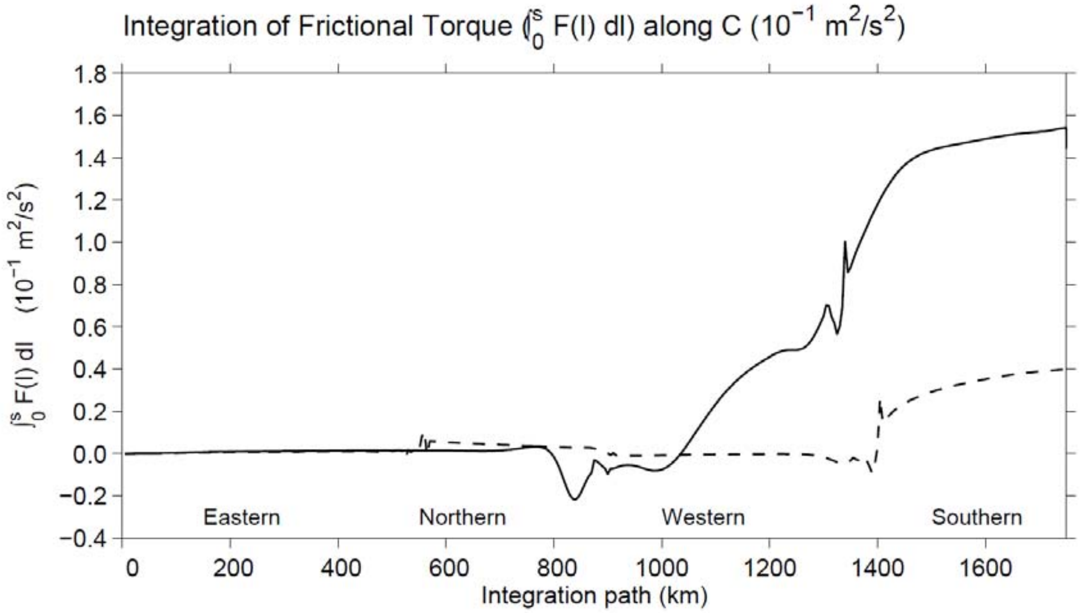

Figure 9: Integration of friction along the isobaths of 1500m in northern basin for IDL-1 (solid line) and IDL-2 (dashed line). The integration starts at the southeastern corner in the northern basin. The increase of the frictional torque is mainly induced by the NIJ-like currents along the southern boundary of the northern basin.

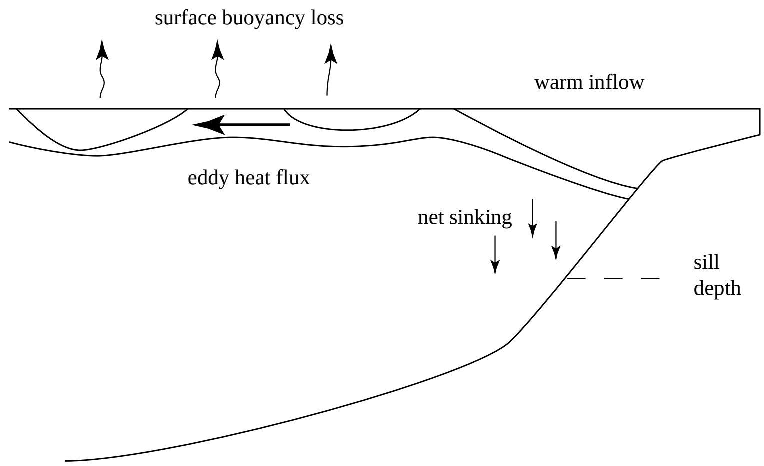

Figure 10: A cartoon that schematizes GCM results from the work of Spall (2003, 2004, and 2010). A warm surface boundary current enters the marginal sea along the right-hand coast. It is baroclinically unstable and sheds warm eddies that disperse into the interior, where they are cooled. The dense water is formed in the interior by convection but the spatially averaged vertical velocity is zero. So the deep outflow is not fed from the interior. There is a return flow of cooler eddies into the boundary current where net sinking preferentially occurs. The implication is that the cold outflow from the marginal sea is fed strictly by the boundary sinking.

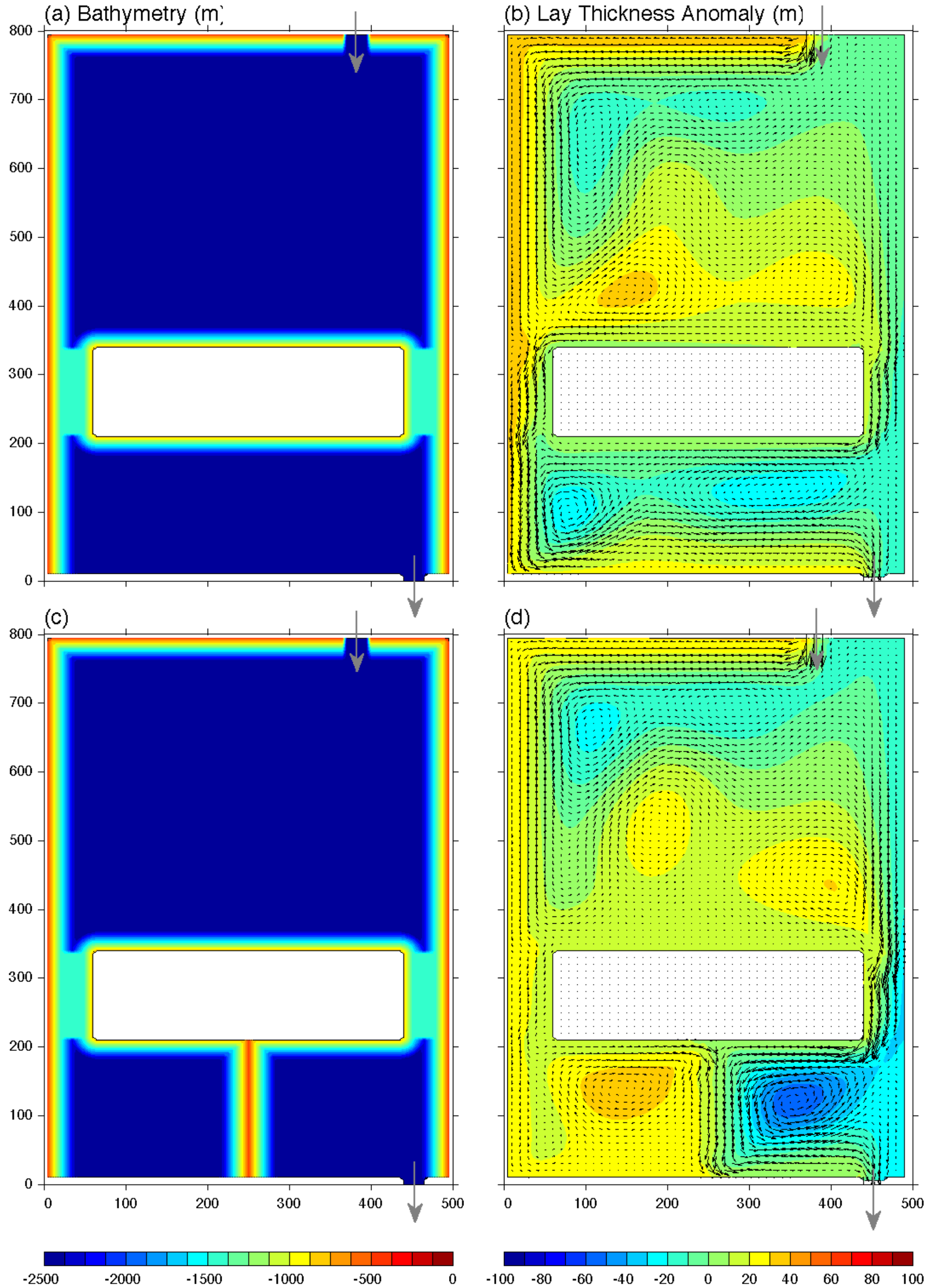

Figure 11: Two idealized experiments (IDL-3 and 4) are designed to elucidate the circulation integral constraint on the existence of the NIJ. The NIJ exists in the IDL-3 (upper panels) because the there exists a closed geostrophic contour that encompasses the island. Along this contour there must be a cyclonic flow to counter the anti-cyclonic overflow through the eastern channel. In the lower panel (IDL-4), such a closed geostrophic contour no longer exists due to an insertion of a ridge in the southern basin. The integral constraint is no longer valid and the NIJ-like current disappears.

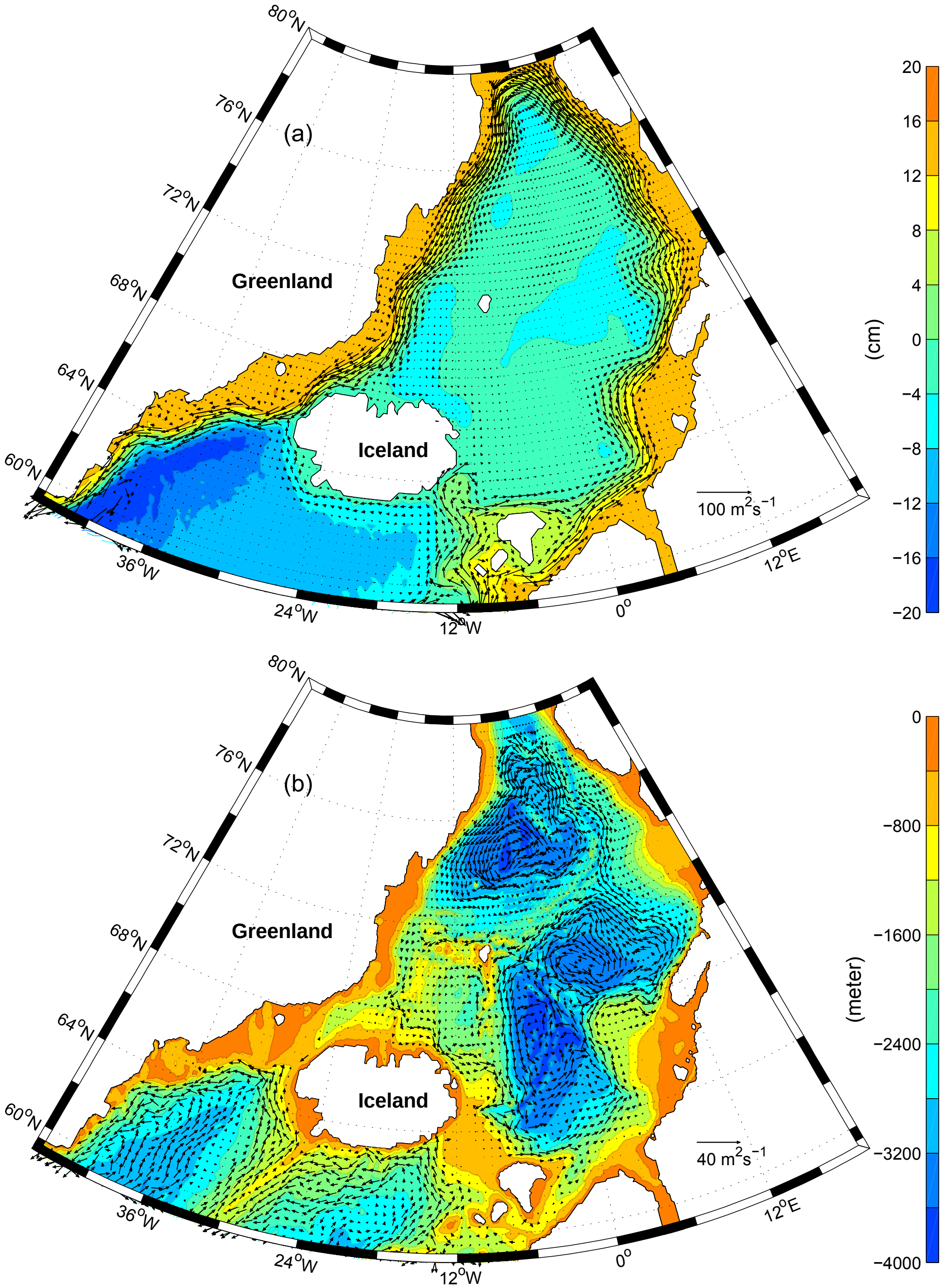

Figure 12: The sea surface height and surface velocity (top panel) and the bathymetry and lower-layer flow (bottom panel). The circulation in the lower layer is cyclonic in the whole Nordic Basin and in each sub-basin. The flow along the north Icelandic shelf and slope is eastward against the NIJ. This implies that wind stress forcing acts against the NIJ.

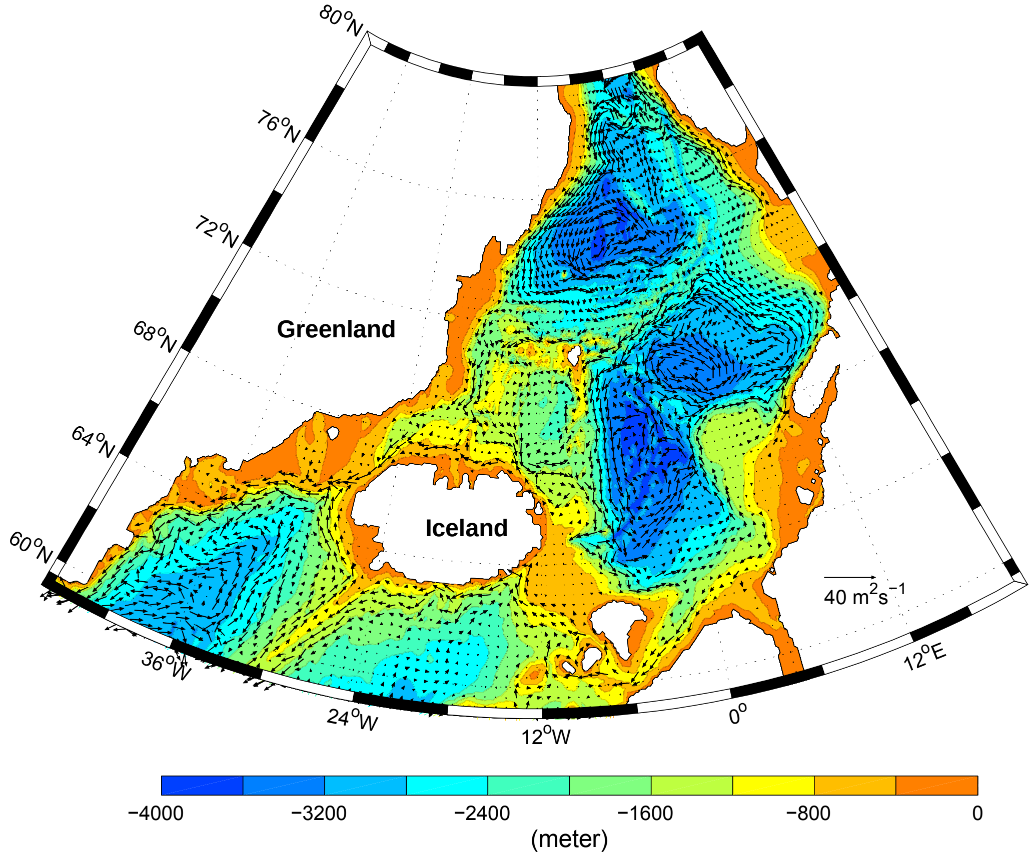

Figure 13: The same as Figure 4b except that the wind stress is applied. The circulation in the overflow layer changes significantly. The EGC pathway is elevated. The flow to the east of the Jan Mayen Ridge is now eastward along the Iceland-Faroe Ridge and becomes the main pathway for the FBC overflow. The flow along the mid-ocean ridges is southward toward the GISR. The circulations in the Nordic Seas are cyclonic. The most relevant feature is that the NIJ still exists robustly along the 600-1000m isobaths toward the Denmark Strait. So the NIJ is not eliminated by wind stress.